

2013

Advanced gel polymer electrolyte for lithium-ion polymer batteries

Ruisi Zhang
Iowa State University

Follow this and additional works at: <https://lib.dr.iastate.edu/etd>

 Part of the [Mechanical Engineering Commons](#)

Recommended Citation

Zhang, Ruisi, "Advanced gel polymer electrolyte for lithium-ion polymer batteries" (2013). *Graduate Theses and Dissertations*. 13515.
<https://lib.dr.iastate.edu/etd/13515>

This Thesis is brought to you for free and open access by the Iowa State University Capstones, Theses and Dissertations at Iowa State University Digital Repository. It has been accepted for inclusion in Graduate Theses and Dissertations by an authorized administrator of Iowa State University Digital Repository. For more information, please contact digirep@iastate.edu.

Advanced gel polymer electrolyte for lithium-ion polymer batteries

by

Ruisi Zhang

A thesis submitted to the graduate faculty

in partial fulfillment of the requirements for the degree of

MASTER OF SCIENCE

Major: Mechanical Engineering

Program of Study Committee:
Reza Montazami, major professor
Pranav Shrotriya
Scott Chumbley
Xinwei Wang

Iowa State University
Ames, Iowa
2013

Copyright © Ruisi Zhang, 2013. All rights reserved.

DEDICATION

This thesis is dedicated to my parents, Jianxun Zhang and Hui Liang, and my grandparents, Daming Zhang, Yingwa Xie, and Shutao Chen.

TABLE OF CONTENTS

	Page
DEDICATION	ii
LIST OF FIGURES	v
LIST OF TABLES	vi
NOMENCLATURE	vii
ACKNOWLEDGEMENTS	viii
ABSTRACT	ix
CHAPTER 1 BACKGROUND AND LITERATURE REVIEW	1
1.1 Introduction	1
1.2 Historical developments in lithium ion battery research	6
1.3 Principle of lithium ion batteries	7
1.4 Design of lithium ion batteries	10
1.5 Anode and cathode	12
1.6 Electrolyte	13
1.7 Gel Polymer Electrolyte	15
1.7.1 Gel Polymer Electrolyte with ionic liquids	17
1.7.2 Gel Polymer Electrolyte with nanomaterials	19
1.8 Summary	19
References	20
CHAPTER 2 MATERIALS AND METHODS	28
2.1 Materials	28
2.2 Synthesis and activation	33
2.2.1 Gel Polymer Electrolyte with ionic liquids	33
2.2.2 Gel Polymer Electrolyte with AuNPs	34
2.3 Lithium ion Polymer Battery Assembly	36
2.3 Measurements	36
References	42

	Page
CHAPTER 3 INFLUENCE OF IONIC LIQUIDS OF THE GEL POLYMER ELECTROLYTE	43
3.1 Introduction	43
3.2 Experimental	47
3.3 Results and discussion.....	48
3.3.1 Ionic Conductivity	48
3.3.2 Interfacial properties	52
3.3.3 Battery performance	56
3.4 Conclusion	59
References	60
CHAPTER 4 INFLUENCE OF GOLD NANOPARTICLES OF THE GEL POLYMER ELECTROLYTE	65
4.1 Introduction	65
4.2 Experimental	67
4.3 Results and discussion.....	69
4.3.1 Property of AuNPs	69
4.3.2 Ionic Conductivity	70
4.3.3 Interfacial properties	72
4.3.4 Battery performance	74
4.4 Conclusion	76
References	77
CHAPTER 5 CONCLUSION AND FUTURE PROPECTIVE.....	80
APPENDIX	83

LIST OF FIGURES

	Page
Figure 1.1 Average price of crude oil from 1945 – 2013 (up to September 2013)	1
Figure 1.2 Burned Li-ion Polymer battery from Boeing 787 Dreamliner	4
Figure 1.3 Schematic of traditional lithium ion battery	8
Figure 1.4 Schematic drawing of various lithium ion battery configurations. a). Cylindrical; b). Coin; c). Thin.....	11
Figure 1.5 Schematic cross-section structure of a thin film lithium ion polymer battery	12
Figure 2.1 Chemical structure of PVdF	28
Figure 2.2 Chemical structure of NMP	29
Figure 2.3 Chemical Structure of EC (left) and PC (right)	30
Figure 2.4 Chemical structure of EMI-TF	30
Figure 2.5 Solvent exchange for AuNPs solutions	31
Figure 2.6 Composite Graphite anode and (LiMn ₂ O ₄) cathode	32
Figure 2.7 GPE fabricate process with ionic liquid	33
Figure 2.8 GPE fabricate process with AuNPs	35
Figure 2.9 Structure of LIPB. Insets on the left show photographic images of the actual structure.....	36
Figure 2.10 VersaSTAT-4	36
Figure 2.11 Ionic Conductivity testing cell.....	37

	Page
Figure 2.12 Setup of impedance spectroscopy	38
Figure 2.13 PerkinElmer Ultraviolet spectroscopy	38
Figure 2.14 Setup of Ultraviolet absorbance spectroscopy	39
Figure 2.15 BST8-MA Battery Analyzer	40
Figure 2.16 Setup of BST8-MA Battery Analyzer	41
Figure 3.1 Bar chart of Ionic conductivity	49
Figure 3.2 Nyquist plots of steel/GPE/steel with different volume percent ionic liquids at high frequency	50
Figure 3.3 Nyquist plots of Graphite/GPE/LiMn ₂ O ₄ with different volume percent ionic liquids	52
Figure 3.4 Equivalent circuit of Lithium-ion polymer cell	55
Figure 3.5 Real impedance verses the radial frequency to the power of (-1/2) at low frequency (63 Hz ~ 3 Hz)	55
Figure 3.6 Consecutive cycling behavior of Graphite/GPE/LiMn ₂ O ₄ systems with different volume percent of ionic liquids	58
Figure 4.1 Comparison of the absorbance	70
Figure 4.2 Comparison of the impedance for steel/GPE/steel with AuNPs and without AuNPs at high frequency	71
Figure 4.3 Equivalent circuit of Lithium-ion polymer cell	72
Figure 4.4 Nyquist plots of CMS/GPE/LiMn ₂ O ₄ with or without AuNPs	74
Figure 4.5 Consecutive cycling behavior of CMS/GPE with or without AuNPs/LiMn ₂ O ₄ systems	76

LIST OF TABLES

	Page
Table 1.1 Capacity factor of different types of power plat	3
Table 2.1 Solvent in volume percent of each group	34
Table 3.1 Values of each term in calculating ionic conductivity	50
Table 3.2 Values of solution resistance and double-layer capacitance in equivalent circuit	56
Table 3.3 The average rest voltages of Graphite/GPE/LiMn ₂ O ₄ systems with different volume percent of ionic liquids after fully charged	58
Table 4.1 Values of each term in calculating ionic conductivity	72

NOMENCLATURE

M	Molecular Weight
ρ	Density
L	Length
W	Width
D	Diameter
σ	Ionic conductivity
t	Thickness
A	Cross-sectional area
R_i	Internal resistance
R_s	Solution resistance
R_{ct}	Charge-transfer resistance
R_b	Bulk resistance
f_m	Medium frequency
f_h	High frequency
f_l	Low frequency
C_{DL}	Double-layer capacitance
$Z_{im,m}$	Medium imaginary impedance
ΔV	Change of voltage
GPE	Gel Polymer Electrolytes
LIPB	Lithium ion polymer battery

AuNPs	Gold Nanoparticles
mm	Millimeter
°C	Degree centigrade

ACKNOWLEDGEMENTS

I would like to thank my major professor, Professor Reza Montazami, and my committee members, Professor Pranav Shrotriya, Professor Scott Chumbley, and Professor Xinwei Wang, for their guidance, help and support throughout this research.

In addition, I would like to thank Dr. Handan Acar, the postdoctoral scientist in our group, for her help and guidance. Also special thanks to Dr. Zhanyou Chi, a postdoctoral research associate for Iowa State's Center for Sustainable Environmental Technologies, for his help and cooperation with my research project.

Moreover, I would like to thank my friends, colleagues, the faculty and staff in the department of Mechanical Engineering for making my time at Iowa State University a wonderful experience; in no particular order, Le Dong, Xinning Xie, Wangyujue Hong, Kevin Osgerby, and Amy Carver.

Finally, thanks to my family for their encouragement and support.

ABSTRACT

In order to keep abreast with the rapid development of portable electronic equipment, improving the performance of polymer electrolytes has therefore become our goal of research. This work improved performance of Li-ion polymer batteries through advanced gel polymer electrolytes (GPEs). Comparing with liquid type Electrolyte, Gel type Polymer Electrolyte (GPE) had the advantage of a wide variety of shape, size and dimensions so that GPE was selected as our target. The GPE is a membrane synthesized by trapping ethylene carbonate, and propylene carbonate in polyvinylidene fluoride and 1-Methyl-2-pyrrolidone solutions.

Advanced GPEs were synthesized by incorporating an organic electrolyte solution (LiPF₆-EC-PC) with ionic liquid (EMI-Tf) into polyvinylidene fluoride-base membranes. Among a series of test including ionic conductivity, film resistance, cell voltage, cyclic voltammetry, and charge/discharge efficiency, 50 volume percent of ionic liquid (EMI-Tf) in an organic electrolyte solution showed the best performance.

We also introduced the nanoparticle-polymer techniques that gold nanoparticles were adding to the GPE membranes as the fillers in order to higher capacity, stronger mechanical strength, and lower internal resistances.

Keywords: GPE, Ionic liquids, Lithium batteries, PVdF, AuNPs

CHAPTER 1

BACKGROUND AND LITERATURE REVIEW

1.1 Introduction and Motivation

According to the first law of thermodynamics, in any isolated system, energy is conserved. That is, energy is neither created nor destroyed, but converted from one form to another. Energy has always been an interesting and critical aspect of human life. Human being has learned to store and convert energy as one of the essential skills of survival. Building dams to store the energy of flowing water, and, hydroelectric turbines to convert mechanical energy of the flowing water to electrical energy are good examples of energy storage and

conversion by humans.

Electricity can be easily transferred from power plants to consumers via power grid; however, more recently need for mobile sources of electrical energy have been increased due

to recent changes in our life styles.

Reliable energy storage is a

critical need for a wide variety of applications such as transportation, notebook computers, portable electronics, medical devices, satellites, spacecraft and elsewhere. In

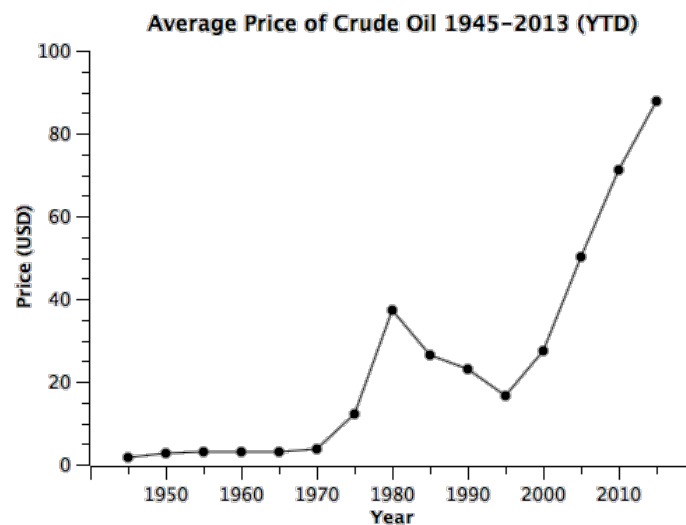


Figure 1.1 Average price of crude oil from 1945 – 2013 (up to September 2013)

Figure is generated based on data from Illinois Oil & Gas Association

most applications, high energy density, high charge/discharge efficiency, cycle durability, time durability, high nominal cell voltage and environmental safety are of significant importance and special interest. Secondary cell batteries have attracted significant attention in the last two decades. There are two main motives behind the increasing attention to secondary cell batteries: 1) portable electronic; and 2) clean energy. As portable electronics are becoming more and more common in our society, and many aspects of our lives are now depended on the performance of our portable electronics, demand for a safe, reliable and efficient mean to store electrical energy for portable devices has increased. Also, recent advances in processing power, screen size and urge for thinner and lighter devices, have increased the demand for lighter batteries with higher energy density. In addition to portable electronics, secondary cell batteries are widely used in hybrid and electric vehicles. Due to environmental concerns and ever-increasing price of fossil-fuels interest on hybrid, and more recently all-electric, vehicles has significantly increased in the U.S. and around the world. According to the U.S. Department of Energy, in 2012 more than 36% of all hybrid and electric vehicles were registered in the U.S. alone. Many automobile companies like Toyota, Hyundai, Honda, Ford and Chevrolet have invested significant resources on development of hybrid and electric vehicles. The price of oil has increased significantly (about 3 folds) in the past two decades (see Figure 1.1), which is directly proportional to the price of fuel for vehicles, airplanes, and fossil-fuel power plants. The increase in the price of fossil-fuels increases the need and urge for a clean and inexpensive alternative sources of energy, such as wind and solar, for transportation, residential and industry sectors. However,

wind and solar energy sources are not continuous sources and along with development of more efficient wind turbines and solar cells, need for research on the storage mechanisms is paramount. According to a report published by the U.S. Energy Information Administration in 2011, capacity factor for wind farms and photovoltaic power plants are 20-40% and 13-19% respectively, depending on the location of the power plant; which are among the lowest capacity factors of power plants (see Table 1.1). Offshore wind farms and photovoltaic power plants located in deserted areas have higher capacity factor. However, it has been demonstrated at commercial level that capacity factor of photovoltaic power plants can be increased to 75% by addition of a power storage mechanism; which will place them at the second highest capacity factor rate among power plants, after nuclear power plants with capacity factor of more than 90%.

Table 1.1 Capacity factor of different types of power plant
Table is generated based on the data reported by the U.S. Energy Information Administration

Plant Type	Average Capacity Factor
Nuclear	90.3%
Solar (with storage)	75%
Coal	63.8%
Hydroelectric	39.8%
Wind	20-40% (vary by location)
Solar	13-19% (vary by location)

Currently, secondary cell batteries are widely used in portable electronics and hybrid and electric vehicles and limitedly for storage of wind and solar energy. Secondary cell batteries have the potential to continue to fulfill the needs for the fast growing energy needs, only if their efficiency can grow accordingly.

Secondary cell batteries can be categorized into two general categories. The first is liquid electrolyte metal-ion batteries where the cell design is cylindrical, and the metal-ion is lithium-ion, sodium-ion and rarely potassium-ion or other metal-ions; whereas the second category is gel polymer electrolyte (GPE) metal-ion batteries (also known as metal-ion polymer batteries) where the electrolyte is gel or solid and the metal-ion is lithium-ion.

Generic AA and AAA rechargeable batteries are among the first category. Battery cells used in hybrid and electric vehicles, smartphones, tablets and most of laptops belong to the second category. Unlike the liquid electrolyte cells that are limited to cylindrical rigid metal cases, metal-ion polymer batteries can have flexible, polymer laminate case of different shapes that allow more freedom in design of the cell for particular applications. In metal-ion polymer batteries the electrode sheet and the separator sheet are laminated onto each other



Figure 1.2 Burned Li-ion Polymer battery from Boeing 787 Dreamliner

Source: Reuters

thus the external pressure, provided by the metal casing in liquid electrolyte metal-ion batteries, is not required. Absence of the heavy metal casing significantly increases the energy density of the battery cell as a whole; thus, metal-ion polymer batteries are preferred for portable electronics and vehicles. For instance, Korean automaker, Hyundai, is using lithium-ion polymer (Li-poly) batteries in its 2012 Sonata Hybrid model with a lifetime battery warranty. Li-poly batteries benefit from a relatively long lifespan and highest cell voltage among secondary cell batteries. Although very efficient and widely used, Li-poly batteries are associated with several issues such as high cost, safety concerns and strict charging/discharging guidelines to prevent damage to the battery cell. Some of these issues are arose from the physical properties of the batteries, such as expansion/contraction while charging and discharging which results in delamination of electrodes, and may also cause damage to the casing and result in exposure of the lithium to the ambient; and some other are due to chemical properties of the materials uses, mainly chemical properties of lithium, such as high reactivity in ambient. Lithium, the backbone of secondary cell batteries, is highly reactive and unstable in ambient. When punctured, Li-poly batteries react quickly and vitally with the moisture in the ambient and may catch on fire. Battery problem of the Boeing 787 Dreamliner is one of the most famous examples of safety issues of Li-poly batteries. Shown in Figure 1.2 is a heavily burned Li-poly battery from the Boeing 787 Dreamliner. Deformation of the protective casing suggests changes in the physical properties of the enclosed battery cells. This particular Li-poly battery consists of eight

battery cells (hard to see from this picture) that are placed in one larger protective cell (the blue box in this picture).

1.2 Historical developments in lithium ion battery research

Primary lithium cell with lithium metal as the anode was first proposed and developed in 1970s [1]. As the lightest metal ($A_r = 6.94 \text{ g.mol}^{-1}$), and the least dense solid ($\rho = 0.534 \text{ g.cm}^{-3}$, with a desirable electron configuration ($1S^2 2S^1$), lithium has great potentials and advantages to be used as the backbone of the metal-ion batteries. In addition, lithium exhibits a -3.04V potential deference against hydrogen electrode, which is desirable for most portable electronic devices. Due to their remarkable advantages including high energy density, high capacity, and variable discharge rate, Lithium cells were rapidly applied in electronic devices, such as watches, calculators, etc. [2] The primary cells are one-off and non-rechargeable power sources, which bring some inconveniency for devices that require high current draw rates. In the 1980s, a large group of scientists put their effort into developing a rechargeable lithium battery, named secondary lithium battery [3]. Additionally, Ennon and Moli Energy made attempts on commercializing the Lithium-Titanium disulfide (Li/TiS_2) system and Lithium-Molybdenum disulfide (Li/MoS_2) system, respectively, which operated at near 2V [4].

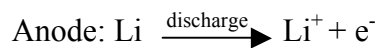
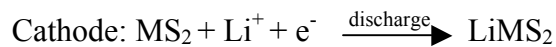
In the earlier models, both primary and secondary lithium batteries were designed based on metallic lithium as positive electrode; however, the interface between lithium metal and electrolyte was not stable since the lithium metal could detach from the surface of the cathode leading to serious safety issue [5-7]. Concerned about safety

issues, lithium metal was replaced by lithiated carbon (graphite and lithium carbonate (LiC_6)) and other lithiated materials (composite alloys and 3d-metal oxides; nitrides) as anodes. Simultaneously, research on cathodes was lead to synthesize metal-oxide cathodes to obtain higher potential, examples include (Li_xMO_2), where M indicated nickel (Ni), cobalt (Co), or manganese (Mn). For the new system, instead of lithium metals, lithium ions rocked back and forth between anode and cathode during charging/discharging process, called rocking-chair system [8]. In June 1991, Sony Corporation commercialized the first rocking-chair battery - graphite-lithium cobalt oxide (C/LiCoO₂) system, which had an open circuit potential (4.2V) and an operation voltage (3.6V) [1].

Since then, a huge wave of research has been focused on all aspects of the lithium-ion batteries including cell design, electrode materials and electrolytes.

1.3 Principle of lithium ion batteries

Primary lithium ion battery is a one-direction device that only has discharging process. During discharging, reduction happens on the cathode gaining electrons and oxidation reacts on the anode losing electrons, displayed in following reaction [9].



(M = Ti or Mo)

In contrast to primary cell batteries, secondary cell lithium-ion batteries are rechargeable. Metal-ion polymer batteries consist of three layers: anode, electrolyte and cathode. The electrochemical properties of the electrode materials strongly depend on the physical and chemical properties like size, homogeneity and surface area. Lithium-ion polymer batteries are by far the most common commercialized secondary cell polymer battery; with leading technology among other types of metal-ion polymer batteries.

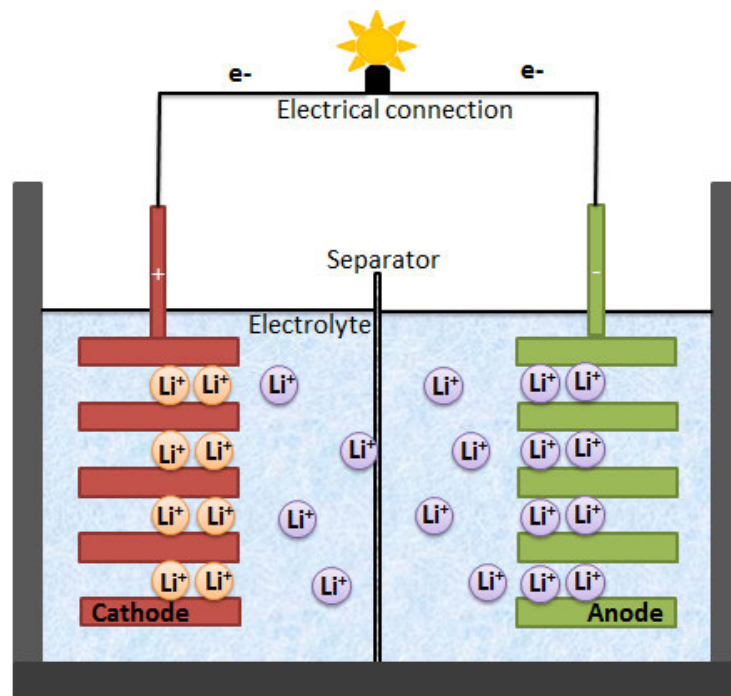


Figure 1.3 Schematic of traditional lithium ion battery

As shown in Figure 1.3, typically, Li-ion polymer batteries are consist of three parts: 1) Positive electrode which commonly consists of LiCoO_2 , [10] LiNiO_2 [11] or LiMn_2O_4 [12] . 2) Separator, which is a conducting gel polymer electrolyte (GPE). GPEs are prepared by immobilization of organic liquid electrolytes into polymer

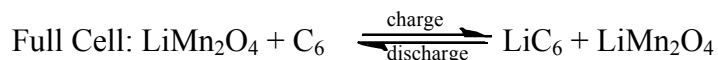
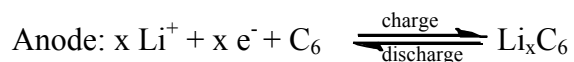
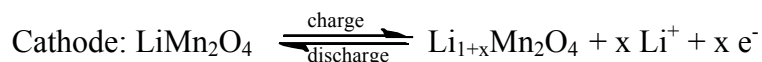
structures[13]. Polymers such as poly(ethylene oxide) (PEO), polyacrylonitrile (PAN), poly(vinylidene fluoride) (PVdF), poly(methyl-methacrylate) (PMMA) are among the well-studied materials[14-17]. 3) Negative electrode which consists of Li or Li-C intercalation compound[18-20]. When charging, lithium ions migrate through electrolyte under a certain external potential from anode to cathode. The discharge process reverses the moving direction of lithium ions; and simultaneously the electrons flow around the external circuit.

Each combination of the abovementioned materials and compound will slightly influence cost, voltage, cycle durability and other characteristics of the Li-poly batteries. What remains unchanged is the safety concern due to instability of lithium. When in contact with water (ambient moisture) lithium, due to its volatile nature, exhibits fast reaction with water that can easily lead to fire and/or explosion[21]. This is not much of a concern in case of consumer electronics as robust casings are developed to protect the battery pouch from damage. However, in case of transportation applications, such as electric/hybrid vehicles the extent of an accident may cause the protective casings to crack or break. As a result a massive fire/explosion may happen. What is concerning in both small-scale (portable electronics) and large-scale (transportation, vehicles and planes) batteries is the expansion/contraction of the cell while charging and discharging; which, over time, causes 1. delamination of electrodes; and 2. physical damage to the casing and possibly exposure of the battery contents to the ambient.

A permanent solution to this problem is to eliminate use of rigid materials in lithium-ion polymer batteries and find a set of alternative soft functional materials for

electrodes and electrolyte that 1) does not require the pressure from casing (thus can be placed in a larger case, taken into account expansion of the materials), and 2) can expand and contract when remain laminated.

There has been an extraordinary work on rocking-chair lithium ion batteries that selected variable materials for electrodes. For instance, Bellcore worked on secondary lithium ion batteries, which $\text{Li}_{1+x}\text{Mn}_2\text{O}_4$ spinel phase was chosen as cathode and graphite as anode [22-24]. During charging/discharging process, the oxidation and reduction process occurred at two electrodes as shown below [25, 26].



The secondary lithium ion batteries, in general, operate 3.7V voltage and demonstrate a capacity of 150mAh/g [27].

1.4 Design of lithium ion batteries

In the earlier days, cylindrical cell configuration (Figure 1.4a) has been the common design for lithium ion batteries [28]. Within the cylinder, all components could be soaked in liquid electrolyte; positive electrode, separator, and current collectors could be rolled around the central cylindrical negative electrode, usually came with carbon. This design saved spaces and maximized the capacity so that it has been one of the most popular cell configurations in the market, especially for primary cell batteries [29, 30].

In order to meet the requirement of portable electronics, such as watches, remote controller, and calculators, etc., smaller, thinner, and lighter design of coin cell (Figure 1.4b) has been developed [31]. The cell can contained anode, separator, and cathode, which were lying from bottom to top and soaking in liquid electrolyte [32].

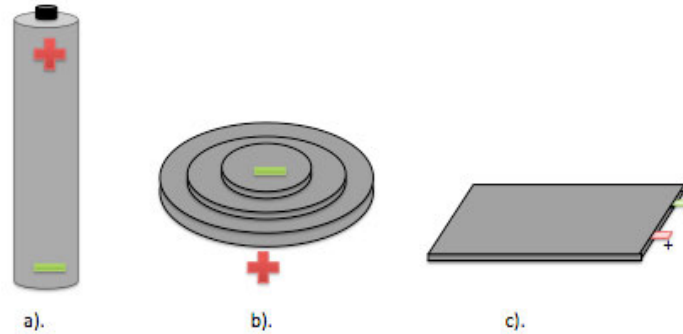


Figure 1.4 Schematic drawing of various lithium ion battery configurations. a). Cylindrical; b). Coin; c). Thin

In 1999, polymer electrolytes replaced the liquid electrolyte in secondary cell lithium ion batteries, which eliminated the shape restriction of cylindrical cell [30]. A thin film polymer battery (Figure 1.4c), with multiple advantages including shape versatility, flexibility, and lightness, was consisted of anode current collector, anode, polymer electrolyte, cathode, and cathode collector [33], a schematic is shown in Figure 1.5. Each part of a thin film lithium ion polymer battery is a thin membrane; some thin film batteries are less than 0.3mm thick [34].

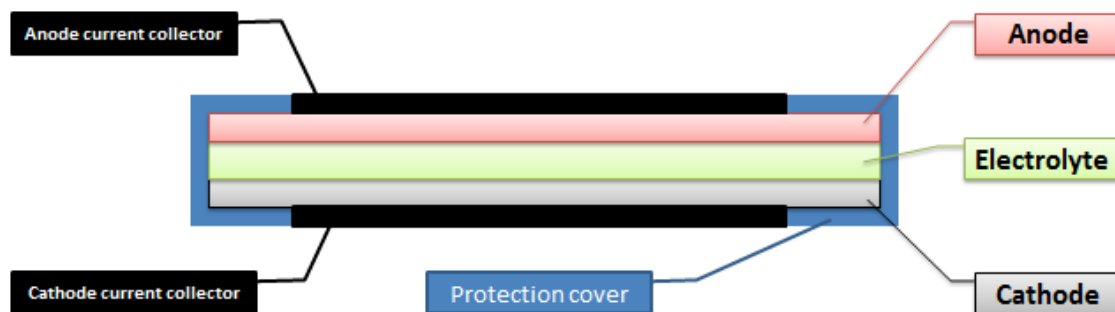


Figure 1.5 Schematic cross-section structure of a thin film lithium ion polymer battery

1.5 Anode and Cathode

Carbonaceous materials, which are able to reversibly intercalate/deintercalate lithium ions into/from the graphite lattice, have been the first choice for anode of lithium ion batteries [35, 36]. Since late 1980s, graphite has been drawn attentions on because of its low redox potential and excellent structural stability [37]. Other non-graphitic carbon, such as soft carbons, carbon nanotubes, and graphene, has also been researched in the recent years [30].

LiCoO_2 was the most common cathode in 1970s, by seeking a more stable, less expensive, and safer material, a few alternatives such as LiNiO_2 , $\text{LiNi}_x\text{Co}_y\text{O}_2$, three-dimensional LiM_2O_4 ($M = \text{Ti}, \text{V}, \text{Mn}$) spinel phase, were synthesized[35, 38]. Comparing with two-dimensional compounds, three-dimensional framework is more stable, the space group of LiM_2O_4 is $\text{Fd}3m$, and enhances the diffusion of lithium ions. Also, LiMn_2O_4 cells could provide around 4V discharge potential versus lithium, so that LiMn_2O_4 became the most common cathode material[39, 40].

1.6 Electrolyte

Electrolyte materials separate anode and cathode and play the significant role of transmitting electrons and lithium ions during charging and discharging processes[41]. Also, electrolyte is one of the key components that define the battery's performance – charging/discharging capacity, safety, cycling performance, and current density. The basic desired qualities of electrolyte materials are listed below [27, 42, 43].

1. High ionic conductivity at wide range of temperatures: increase the lithium ions diffusion and resist polarization during charging/discharging
2. Good thermal stability: ensures the battery operation under appropriate temperature
3. Wide electrochemical window: prevents side reactions between electrodes and electrolyte
4. Good mechanical property: ease of manufacturing and enhanced safety
5. Low cost
6. Safety: high flashing point
7. Non-toxic: environmental friendly

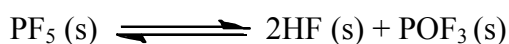
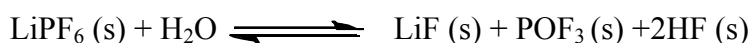
Depending on the physical state of electrolyte, electrolytes can be divided into three major categories: liquid electrolyte, solid electrolyte, and gel electrolyte.

Most primary cell lithium ion batteries and some secondary cell lithium ion batteries are designed based on liquid electrolytes, containing a lithium salt, such as LiPF_6 , LiBF_6 , LiClO_4 , LiBC_4O_8 , or $\text{Li}[\text{PF}_3(\text{C}_2\text{CF}_5)_3]$, dissolved in organic alkyl carbonate solvent. Due to low interfacial resistance, low cost and ease of synthesis,

LiClO₄ was the most common lithium salts used in the earlier designs. However, the high oxidability of anions (ClO₄⁻) caused some safety issue; thus LiPF₆ replaced LiClO₄ in the newer designs and became the major material for electrolytes, which exhibits better overall performance including higher ionic conductivity. One of the shortcomings of LiPF₆ is the low thermal stability compare to other lithium salts. LiPF₆ can decompose at 80°C in the following way [44].



The PF₅ gas has a high Lewis acidity, which leads to side reactions between PF₅ gas and solvent and increases the internal pressure of the cell. Meanwhile, LiPF₆ is very sensitive to moisture and react with H₂O as shown below [45].



LiF is barely conductive so it will increase the interfacial resistance on the surface of the electrodes [46]. In order to control the level of moisture and minimize the side reaction during manufacturing the batteries, it has become necessary that every process involving LiPF₆ be carried under a close environment of inert gasses with low (preferably 0) moisture content.

Since commercial Li-ion batteries use LiPF₆ as lithium salt, and as mentioned above LiPF₆ is sensitive to H₂O, it requires a non-aqueous solvent to improve the performance and safety of the battery, an organic alkyl carbonate can be a suitable solvent [47, 48]. The most common organic alkyl carbonate solvents are one or mixture of the following: propylene carbonate (PC), ethylene carbonate (EC), diethyl carbonate

(DEC), dimethyl carbonate (DMC), or ethyl methyl carbonate (EMC). The cyclic carbonates, PC and EC, have high dielectric constant ($\epsilon(\text{EC at } 40^\circ\text{C})=89.78$ and $\epsilon(\text{PC at } 25^\circ\text{C})=64.92$), which is a significant feature for dissolution of lithium salt, and high flash point ($\text{FP}(\text{EC})=150^\circ\text{C}$ and $\text{FP}(\text{PC})=132^\circ\text{C}$), which is an important factor for the safety of the cells[49]. According to Li *et al*, a mixture of EC and PC could dissolve larger amount of lithium salt compare to other possible mixtures[50].

Instead of a liquid electrolyte, using a polymer overcomes the constraint of cell configuration and make thin film lithium ion polymer batteries possible. For the solid electrolyte, the lithium salt is containing in the polymer membrane, such as Polyethylene oxide (PEO) containing LiPF_6 [27, 34, 51]. Both solid electrolyte and gel electrolyte are using polymer membrane as a host matrix, but the difference between solid electrolyte and gel electrolyte is the solvent content. Gel electrolytes are synthesized by incorporating liquid electrolyte into polymer base membranes by soaking membranes in lithium-based organic electrolytes.

1.7 Gel Polymer Electrolyte

Comparing to solid electrolytes and liquid electrolytes, Gel polymer electrolytes (GPEs) have several advantages, including no shape restrictions, faster charging/discharging, and higher power density [42, 52, 53]. Currently, there are four major polymer host materials for GPEs: polyethylene oxide (PEO), polyacrylonitrile (PAN), polymethyl methacrylate (PMMA), and polyvinylidene fluoride (PVdF) [42].

In the past two decades, PEO-based electrolytes were the major polymer host matrix used in batteries; and significant research efforts have been placed on their development and improvement. The conduction of PEO-based gel polymer electrolytes is mainly through the complexes between lithium-ion and ether oxygen atom [54]. PEO-based electrolyte is the first studied system, which could be easily casted as thin membranes. However, due to PEO's high degree of crystallinity, the ionic conductivity of PEO-based electrolytes is low and varies from 10^{-8} S cm⁻¹ to 10^{-4} S cm⁻¹ at temperature between 40°C and 100°C [53]. Ito *et al* observed that the ionic conductivity increases as the plasticizer increases, but the interfacial properties become worse due to the presence of hydroxyl end-groups [55].

In the later studies PAN was used as the electrolyte host matrix material because of its small thermal resistance and flame-retardant property. According to Feuliade *et al*, the ionic conductivity of PAN-based gel electrolyte is between 10^{-5} S cm⁻¹ and 10^{-3} S cm⁻¹; and the amount of transferred lithium ion is larger than PEO-based gel polymer electrolyte [56]. The negative side of PAN-based GPE is the increasing internal resistance of the lithium-ion polymer battery. Choi *et al* observed that combining PAN and PEO together, which is (10PEO-40PAN-12LiClO₄-38EC/BL), could improve the mechanical flexibility, ionic conductivity, and interfacial properties of GPE [57].

PMMA-based GPEs are also used due to their enhanced interface stability and lower cost, due to rich raw materials and simple synthesis process, among other host matrix materials. However, its poor mechanical flexibility narrowed down the applications. Copolymerization between PMMA and other polymer provides better

performance to lithium-ion polymer battery. As Ramesh *et al* showed, PVC copolymerized with PMMA could increase the conductivity of GPEs [58]. According to Lee *et al*, porous PDMS-CNT nanocomposites with PMMA could improve the flexibility and successfully control the degree of phase separation between PDMS and PMMA [59].

Recently, the most common polymer used in today's lithium-ion polymer batteries is PVdF, containing strong electron-withdrawing functional groups (-C-F) to induce a net dipole moment [60]. PVdF also have a high dielectric constant ($\epsilon = 8.4$) that supports high concentration of charge carriers. Cheo *et al* found that PVdF-PC-LiN(SO₂CF₃)₂ electrolyte system could offer ionic conductivity of 1.74×10^{-3} S/cm[61]. Due to the semi-crystalline structure of PVdF, lithium ions are drafted into the PVdF membrane when they stay on the surface [62-66]. Thus, a gel polymer electrolyte membrane with fully interconnected open microspores, i.e. higher interfacial surface area, enhances ion storage and mobility [13, 64, 67-70]. Although the mobility of PVdF-based GPEs is greater than other polymer host matrix materials, the ionic conductivity of GPEs is still lower than liquid electrolytes. Introducing ionic liquids or nanosize fillers in GPE system could help to improve the performance of lithium-ion polymer batteries.

1.6.1 Gel Polymer Electrolytes with ionic liquids

Application of ionic liquids in lithium-ion batteries has been focus of several studies in the recent years. Fernicaola *et al*, incorporated ionic liquids in an organic electrolyte solution to increase the ionic conductivity and stabilize the lithium ions

carried on the surface of PVdF-base membrane [71]. In one study Egashira *et al* have shown that the ion mobility through the GPE containing ionic liquids depends on the miscibility of polymer component in the ionic liquid.

Among aprotic ILs, protic ILs, and Zwitter ILs, the aprotic class of ILs with high mobility and ion concentration stands out for advanced electrochemical systems, which consist of large irregular cations and small anions[72]. Balducci, *et al* reported the aprotic IL, 1-*n*- Butyl-3-methylimidazolium hexafluorophosphate (BMIPF₆), used in activated carbon/poly(3-methyl-thiophene) hybrid super-capacitor and improved the voltage and cycle life of the super-capacitor [73]. For lithium batteries, Sakaebe *et al* studied and compared a few room temperature ionic liquid containing quaternary ammonium cation and imide anion and concluded that quaternary ammonium cations, including EMI (1-ethyl-3-methylimidazolium) cation, TMPA (trimethylpropylammonium) cation, P13 (N-methyl-N-propylpyridinium) cation, PP13 (N-methyl-N-propylpiperidinium) cation and TFSI (bis(trifluoromethanesulfonyl)imide) cation, could stabilize the reduction on the lithium metal [74]. Furthermore, Fuller *et al* demonstrated that 1-ethyl-3-methylimidazolium tetrafluoroborate (EMIBF₄) as an electrolyte solvent for LiBF₄ operate high charge and discharge potentials, 1.46V and 1.05V with the electrode of Li_xCoO₂ and -2.81V and -2.52V with the electrode of β-LiAl, due to its desirable properties including high ionic conductivity, a wide electrochemical window, and thermal stability [75]. Based on the study from McEwen *et al*, the acidic proton in C-2 on the imidazolium ring might cause poor stability of reduction [76]. Fung *et al* studied with the addition of C₆H₅SO₂Cl could stabilize the

reaction happened on the surface of electrode [77]. Overall, room temperature ionic liquids could improve the performance of lithium ion polymer battery [73, 75, 77].

1.6.2 Gel Polymer Electrolytes with nanomaterials

PG Bruce *et al.* reported nanomaterials could increase the rate of lithium insertion/removal, enhance the electron transport within the particles, and change the electrode potentials, but nanomaterials might cause more side reactions and increase the energy density [78-80]. Yang *et al.* demonstrated the ceramic fillers in PVdF-based gel polymer electrolytes improves interfacial stability between the electrode and the electrolyte, especially the cells with Al₂O₃ fillers that capacity remained 95% of the initial capacity after 100 cycles at a C/2 rate [81]. In order to increase the ionic conductivity of GPEs in the meantime, metallic nanoparticles can be used in synthesis the PVdF-based membrane. Metallic nanoparticles, mainly gold nanoparticles, are commonly used in diagnostics, sensors and other electronic devices, owing to the high stability and conductivity of gold[82].

1.7 Summary

This work is focused on improving the performance of lithium ion polymer batteries by introducing ionic liquids and gold nanoparticles in GPEs. Chapter 3 will discuss the influence of concentration of ionic liquids in electrolyte solutions; and Chapter 4 will discuss the influence of gold nanoparticles on the performance of GPEs.

REFERENCES

- [1] J. M. Tarascon and M. Armand, "Issues and challenges facing rechargeable lithium batteries," *Nature*, vol. 414, pp. 359-367, 2001.
- [2] A. Patil, V. Patil, D. Wook Shin, J.-W. Choi, D.-S. Paik, and S.-J. Yoon, "Issue and challenges facing rechargeable thin film lithium batteries," *Materials research bulletin*, vol. 43, pp. 1913-1942, 2008.
- [3] D. Wainwright, "Battery incorporating hydraulic activation of disconnect safety device on overcharge," ed: Google Patents, 1995.
- [4] J. S. Lundsgaard, "Electrochemical cell," ed: Google Patents, 1989.
- [5] J. Besenhard and G. Eichinger, "High energy density lithium cells: Part I. Electrolytes and anodes," *Journal of Electroanalytical Chemistry and Interfacial Electrochemistry*, vol. 68, pp. 1-18, 1976.
- [6] J.-P. Gabano, "Lithium batteries," *London and New York, Academic Press, 1983, 467 p.*, vol. 1, 1983.
- [7] D. Murphy, P. Christian, F. DiSalvo, and J. Waszczak, "Lithium incorporation by vanadium pentoxide," *Inorganic Chemistry*, vol. 18, pp. 2800-2803, 1979.
- [8] J. Tarascon and D. Guyomard, "The $\text{Li}_{1+x}\text{Mn}_2\text{O}_4/\text{C}$ rocking-chair system: a review," *Electrochimica Acta*, vol. 38, pp. 1221-1231, 1993.
- [9] M. S. Whittingham, "Lithium batteries and cathode materials," *Chemical Reviews*, vol. 104, pp. 4271-4302, 2004.
- [10] Z. Chen and J. R. Dahn, "Methods to obtain excellent capacity retention in LiCoO_2 cycled to 4.5 V," *ELECTROCHIMICA ACTA*, vol. 49, pp. 1079-1090, 2004.
- [11] J. Maruta, H. Yasuda, and M. Yamachi, "Low-temperature synthesis of lithium nickelate positive active material from nickel hydroxide for lithium cells," *Journal of Power Sources*, vol. 90, pp. 89-94, 2000.
- [12] X. He, J. Li, Y. Cai, C. Jiang, and C. Wan, "Preparation of spherical spinel LiMn_2O_4 cathode material for Li-ion batteries," *Materials Chemistry and Physics*, vol. 95, pp. 105-108, 2006.

- [13] Y. Wang, J. Travas-Sejdic, and R. Steiner, "Polymer gel electrolyte supported with microporous polyolefin membranes for lithium ion polymer battery," *Solid State Ionics*, vol. 148, pp. 443-449, 2002.
- [14] K. M. Abraham and M. Alamgir, "Room temperature polymer electrolytes and batteries based on them," *Solid State Ionics*, vol. 70–71, Part 1, pp. 20-26, 1994.
- [15] H. C. Shiao, D. Chua, H.-p. Lin, S. Slane, and M. Salomon, "Low temperature electrolytes for Li-ion PVDF cells," *Journal of Power Sources*, vol. 87, pp. 167-173, 2000.
- [16] K. Murata, S. Izuchi, and Y. Yoshihisa, "An overview of the research and development of solid polymer electrolyte batteries," *ELECTROCHIMICA ACTA*, vol. 45, pp. 1501-1508, 2000.
- [17] S. Panero and B. Scrosati, "Gelification of liquid–polymer systems: a valid approach for the development of various types of polymer electrolyte membranes," *Journal of Power Sources*, vol. 90, pp. 13-19, 2000.
- [18] J. B. Goodenough and Y. Kim, "Challenges for Rechargeable Li Batteries†," *CHEMISTRY OF MATERIALS*, vol. 22, pp. 587-603, 2009.
- [19] B. Key, R. Bhattacharyya, M. Morcrette, V. Seznéc, J.-M. Tarascon, and C. P. Grey, "Real-time NMR investigations of structural changes in silicon electrodes for lithium-ion batteries," *JOURNAL OF THE AMERICAN CHEMICAL SOCIETY*, vol. 131, pp. 9239-9249, 2009.
- [20] S.-H. Yeon, K.-N. Jung, S. Yoon, K.-H. Shin, and C.-S. Jin, "Electrochemical performance of carbide-derived carbon anodes for lithium-ion batteries," *Journal of Physics and Chemistry of Solids*, 2013.
- [21] Q. Wang, P. Ping, X. Zhao, G. Chu, J. Sun, and C. Chen, "Thermal runaway caused fire and explosion of lithium ion battery," *Journal of Power Sources*, vol. 208, pp. 210-224, 2012.
- [22] D. Guyomard and J. Tarascon, "Li Metal - Free Rechargeable LiMn₂O₄/Carbon Cells: Their Understanding and Optimization," *Journal of The Electrochemical Society*, vol. 139, pp. 937-948, 1992.
- [23] J. Tarascon and D. Guyomard, "Li Metal - Free Rechargeable Batteries Based on Li_{1+x}Mn₂O₄ Cathodes (0 ≤ x ≤ 1) and Carbon Anodes," *Journal of The Electrochemical Society*, vol. 138, pp. 2864-2868, 1991.
- [24] J. Tarascon, W. McKinnon, F. Coowar, T. Bowmer, G. Amatucci, and D. Guyomard, "Synthesis Conditions and Oxygen Stoichiometry Effects on Li

- Insertion into the Spinel LiMn_2O_4 ," *Journal of The Electrochemical Society*, vol. 141, pp. 1421-1431, 1994.
- [25] S. Chitra, P. Kalyani, T. Mohan, R. Gangadharan, B. Yebka, S. Castro-Garcia, M. Massot, C. Julien, and M. Eddrief, "Characterization and electrochemical studies of LiMn_2O_4 cathode materials prepared by combustion method," *Journal of electroceramics*, vol. 3, pp. 433-441, 1999.
- [26] X. Li, F. Cheng, B. Guo, and J. Chen, "Template-synthesized LiCoO_2 , LiMn_2O_4 , and $\text{LiNi}_{0.8}\text{Co}_{0.2}\text{O}_2$ nanotubes as the cathode materials of lithium ion batteries," *The Journal of Physical Chemistry B*, vol. 109, pp. 14017-14024, 2005.
- [27] J.-M. Tarascon and M. Armand, "Issues and challenges facing rechargeable lithium batteries," *Nature*, vol. 414, pp. 359-367, 2001.
- [28] K. Nakai, T. Nakano, and K. Hironaka, "Cylindrical lithium-ion battery," ed: Google Patents, 2003.
- [29] K. Nakai, T. Nakano, and K. Hironaka, "Cylindrical lithium-ion battery," ed: EP Patent 1,102,342, 2012.
- [30] M. Wakihara, "Recent developments in lithium ion batteries," *Materials Science and Engineering: R: Reports*, vol. 33, pp. 109-134, 2001.
- [31] S. Park, A. Savvides, and M. Srivastava, "Battery capacity measurement and analysis using lithium coin cell battery," in *Proceedings of the 2001 international symposium on Low power electronics and design*, 2001, pp. 382-387.
- [32] J. Dahn, U. Von Sacken, M. Juzkow, and H. Al - Janaby, "Rechargeable LiNiO_2 /carbon cells," *Journal of The Electrochemical Society*, vol. 138, pp. 2207-2211, 1991.
- [33] J. L. Souquet and M. Duclot, "Thin film lithium batteries," *Solid State Ionics*, vol. 148, pp. 375-379, 2002.
- [34] W. H. Meyer, "Polymer Electrolytes for Lithium - Ion Batteries," *Advanced materials*, vol. 10, pp. 439-448, 1998.
- [35] R. Kanno, Y. Takeda, T. Ichikawa, K. Nakanishi, and O. Yamamoto, "Carbon as negative electrodes in lithium secondary cells," *Journal of Power Sources*, vol. 26, pp. 535-543, 1989.
- [36] M. Mohri, N. Yanagisawa, Y. Tajima, H. Tanaka, T. Mitate, S. Nakajima, M. Yoshida, Y. Yoshimoto, T. Suzuki, and H. Wada, "Rechargeable lithium battery

- based on pyrolytic carbon as a negative electrode," *Journal of Power Sources*, vol. 26, pp. 545-551, 1989.
- [37] E. Peled, C. Menachem, D. Bar - Tow, and A. Melman, "Improved Graphite Anode for Lithium - Ion Batteries Chemically Bonded Solid Electrolyte Interface and Nanochannel Formation," *Journal of The Electrochemical Society*, vol. 143, pp. L4-L7, 1996.
- [38] S. Iijima, "Direct observation of the tetrahedral bonding in graphitized carbon black by high resolution electron microscopy," *Journal of Crystal Growth*, vol. 50, pp. 675-683, 1980.
- [39] G. Amatucci and J.-M. Tarascon, "Optimization of Insertion Compounds Such as LiMn_2O_4 for Li-Ion Batteries," *Journal of The Electrochemical Society*, vol. 149, pp. K31-K46, 2002.
- [40] J. Tarascon, D. Guyomard, and G. Baker, "An update of the Li metal-free rechargeable battery based on $\text{Li}_{1+x}\text{Mn}_2\text{O}_4$ cathodes and carbon anodes," *Journal of Power Sources*, vol. 44, pp. 689-700, 1993.
- [41] W. van Schalkwijk and B. Scrosati, *Advances in lithium-ion batteries*: Springer, 2002.
- [42] M. Armand and J.-M. Tarascon, "Building better batteries," *Nature*, vol. 451, pp. 652-657, 2008.
- [43] K. Xu, "Nonaqueous liquid electrolytes for lithium-based rechargeable batteries," *Chemical Reviews*, vol. 104, pp. 4303-4418, 2004.
- [44] S. E. Sloop, J. K. Pugh, S. Wang, J. Kerr, and K. Kinoshita, "Chemical Reactivity of PF_5 and LiPF_6 in Ethylene Carbonate/Dimethyl Carbonate Solutions," *Electrochemical and Solid-State Letters*, vol. 4, pp. A42-A44, 2001.
- [45] C. Barlowz, "Reaction of Water with Hexafluorophosphates and with Li Bis (perfluoroethylsulfonyl) imide Salt," *Electrochemical and Solid-State Letters*, vol. 2, pp. 362-364, 1999.
- [46] K. M. Abraham, "Directions in secondary lithium battery research and development," *Electrochimica Acta*, vol. 38, pp. 1233-1248, 1993.
- [47] T. Kawamura, A. Kimura, M. Egashira, S. Okada, and J.-I. Yamaki, "Thermal stability of alkyl carbonate mixed-solvent electrolytes for lithium ion cells," *Journal of Power Sources*, vol. 104, pp. 260-264, 2002.

- [48] B. D. McCloskey, D. S. Bethune, R. M. Shelby, G. Girishkumar, and A. C. Luntz, "Solvents' Critical Role in Nonaqueous Lithium–Oxygen Battery Electrochemistry," *The Journal of Physical Chemistry Letters*, vol. 2, pp. 1161-1166, 2011/05/19 2011.
- [49] T. Tamura, K. Yoshida, T. Hachida, M. Tsuchiya, M. Nakamura, Y. Kazue, N. Tachikawa, K. Dokko, and M. Watanabe, "Physicochemical properties of glyme–Li salt complexes as a new family of room-temperature ionic liquids," *Chemistry Letters*, vol. 39, pp. 753-755, 2010.
- [50] T. Li and P. B. Balbuena, "Theoretical studies of lithium perchlorate in ethylene carbonate, propylene carbonate, and their mixtures," *Journal of The Electrochemical Society*, vol. 146, pp. 3613-3622, 1999.
- [51] F. Croce, G. Appetecchi, L. Persi, and B. Scrosati, "Nanocomposite polymer electrolytes for lithium batteries," *Nature*, vol. 394, pp. 456-458, 1998.
- [52] A. Manuel Stephan, "Review on gel polymer electrolytes for lithium batteries," *European Polymer Journal*, vol. 42, pp. 21-42, 2006.
- [53] J. Song, Y. Wang, and C. Wan, "Review of gel-type polymer electrolytes for lithium-ion batteries," *Journal of Power Sources*, vol. 77, pp. 183-197, 1999.
- [54] P. G. Bruce, "Structure and electrochemistry of polymer electrolytes," *Electrochimica Acta*, vol. 40, pp. 2077-2085, 1995.
- [55] Y. Ito, K. Kanehori, K. Miyauchi, and T. Kudo, "Ionic conductivity of electrolytes formed from PEO-LiCF₃SO₃ complex low molecular weight poly (ethylene glycol)," *Journal of materials science*, vol. 22, pp. 1845-1849, 1987.
- [56] G. Feuillade and P. Perche, "Ion-conductive macromolecular gels and membranes for solid lithium cells," *Journal of Applied Electrochemistry*, vol. 5, pp. 63-69, 1975.
- [57] B. Choi, Y. Kim, and H. Shin, "Ionic conduction in PEO–PAN blend polymer electrolytes," *Electrochimica Acta*, vol. 45, pp. 1371-1374, 2000.
- [58] S. Ramesh, K. H. Leen, K. Kumutha, and A. Arof, "FTIR studies of PVC/PMMA blend based polymer electrolytes," *Spectrochimica Acta Part A: Molecular and Biomolecular Spectroscopy*, vol. 66, pp. 1237-1242, 2007.
- [59] H. Lee, J. K. Yoo, J. H. Park, J. H. Kim, K. Kang, and Y. S. Jung, "A Stretchable Polymer–Carbon Nanotube Composite Electrode for Flexible Lithium - Ion Batteries: Porosity Engineering by Controlled Phase Separation," *Advanced Energy Materials*, vol. 2, pp. 976-982, 2012.

- [60] D. M. Esterly, "Manufacturing of Poly (vinylidene fluoride) and Evaluation of its Mechanical Properties," 2002.
- [61] H. Choe, J. Giaccai, M. Alamgir, and K. Abraham, "Preparation and characterization of poly (vinyl sulfone)-and poly (vinylidene fluoride)-based electrolytes," *Electrochimica Acta*, vol. 40, pp. 2289-2293, 1995.
- [62] V. Gentili, S. Panero, P. Reale, and B. Scrosati, "Composite gel-type polymer electrolytes for advanced, rechargeable lithium batteries," *Journal of Power Sources*, vol. 170, pp. 185-190, 2007.
- [63] A. Salimi and A. A. Yousefi, "Analysis Method: FTIR studies of β -phase crystal formation in stretched PVDF films," *Polymer Testing*, vol. 22, pp. 699-704, 2003.
- [64] J. R. Kim, S. W. Choi, S. M. Jo, W. S. Lee, and B. C. Kim, "Electrospun PVdF-based fibrous polymer electrolytes for lithium ion polymer batteries," *Electrochimica Acta*, vol. 50, pp. 69-75, 2004.
- [65] H. P. Zhang, P. Zhang, Z. H. Li, M. Sun, Y. P. Wu, and H. Q. Wu, "A novel sandwiched membrane as polymer electrolyte for lithium ion battery," *Electrochemistry Communications*, vol. 9, pp. 1700-1703, 2007.
- [66] G.-L. Ji, B.-K. Zhu, Z.-Y. Cui, C.-F. Zhang, and Y.-Y. Xu, "PVDF porous matrix with controlled microstructure prepared by TIPS process as polymer electrolyte for lithium ion battery," *Polymer*, vol. 48, pp. 6415-6425, 2007.
- [67] F. Boudin, X. Andrieu, C. Jehoulet, and I. I. Olsen, "Microporous PVdF gel for lithium-ion batteries," *Journal of Power Sources*, vol. 81-82, pp. 804-807, 1999.
- [68] S. W. Choi, S. M. Jo, W. S. Lee, and Y. R. Kim, "An Electrospun Poly(vinylidene fluoride) Nanofibrous Membrane and Its Battery Applications," *Advanced Materials*, vol. 15, pp. 2027-2032, 2003.
- [69] R. Montazami, S. Liu, Y. Liu, D. Wang, Q. Zhang, and J. R. Heflin, "Thickness dependence of curvature, strain, and response time in ionic electroactive polymer actuators fabricated via layer-by-layer assembly," *JOURNAL OF APPLIED PHYSICS*, vol. 109, p. 104301, 2011.
- [70] R. Montazami, D. Wang, and J. R. Heflin, "Influence of conductive network composite structure on the electromechanical performance of ionic electroactive polymer actuators," *International Journal of Smart and Nano Materials*, vol. 3, pp. 204-213, 2012.

- [71] A. Fericola, B. Scrosati, and H. Ohno, "Potentialities of ionic liquids as new electrolyte media in advanced electrochemical devices," *Ionics*, vol. 12, pp. 95-102, 2006.
- [72] H. Matsumoto, H. Sakaebe, K. Tatsumi, M. Kikuta, E. Ishiko, and M. Kono, "Fast cycling of Li/LiCoO₂ cell with low-viscosity ionic liquids based on bis (fluorosulfonyl) imide [FSI]," *Journal of Power Sources*, vol. 160, pp. 1308-1313, 2006.
- [73] A. Balducci, F. Soavi, and M. Mastragostino, "The use of ionic liquids as solvent-free green electrolytes for hybrid supercapacitors," *Applied Physics A*, vol. 82, pp. 627-632, 2006.
- [74] H. Sakaebe and H. Matsumoto, "N-Methyl-N-propylpiperidinium bis (trifluoromethanesulfonyl) imide (PP13-TFSI)—novel electrolyte base for Li battery," *Electrochemistry Communications*, vol. 5, pp. 594-598, 2003.
- [75] J. Fuller, R. T. Carlin, and R. A. Osteryoung, "The Room Temperature Ionic Liquid 1 - Ethyl - 3 - methylimidazolium Tetrafluoroborate: Electrochemical Couples and Physical Properties," *Journal of The Electrochemical Society*, vol. 144, pp. 3881-3886, 1997.
- [76] A. B. McEwen, H. L. Ngo, K. LeCompte, and J. L. Goldman, "Electrochemical properties of imidazolium salt electrolytes for electrochemical capacitor applications," *Journal of The Electrochemical Society*, vol. 146, pp. 1687-1695, 1999.
- [77] Y. Fung and R. Zhou, "Room temperature molten salt as medium for lithium battery," *Journal of Power Sources*, vol. 81, pp. 891-895, 1999.
- [78] P. G. Bruce, B. Scrosati, and J. M. Tarascon, "Nanomaterials for rechargeable lithium batteries," *Angewandte Chemie International Edition*, vol. 47, pp. 2930-2946, 2008.
- [79] A. Subramania, N. T. Kalyana Sundaram, A. R. Sathiya Priya, and G. Vijaya Kumar, "Preparation of a novel composite micro-porous polymer electrolyte membrane for high performance Li-ion battery," *Journal of Membrane Science*, vol. 294, pp. 8-15, 2007.
- [80] P. Balaya, A. J. Bhattacharyya, J. Jamnik, Y. F. Zhukovskii, E. A. Kotomin, and J. Maier, "Nano-ionics in the context of lithium batteries," *Journal of Power Sources*, vol. 159, pp. 171-178, 2006.

- [81] C.-M. Yang, H.-S. Kim, B.-K. Na, K.-S. Kum, and B. W. Cho, "Gel-type polymer electrolytes with different types of ceramic fillers and lithium salts for lithium-ion polymer batteries," *Journal of Power Sources*, vol. 156, pp. 574-580, 2006.
- [82] J. Shan and H. Tenhu, "Recent advances in polymer protected gold nanoparticles: synthesis, properties and applications," *Chemical Communications*, pp. 4580-4598, 2007.

CHAPTER 2

MATERIALS AND METHODS

This chapter discusses the materials, techniques, synthesis and activation procedures, battery assembly and measurements involved in this research on lithium ion polymer batteries. Section 2.1 provides information on materials including the chemical properties, chemical structure, and preparation processes. Section 2.2 discusses the details of synthesis and activation processes of Gel Polymer Electrolytes (GPE). Detailed assembly process of lithium ion polymer batteries is discussed in Section 2.3. Finally, the related techniques and equipment used in measurements, recording and analysis of the data are discussed in Section 2.4.

2.1 Materials

PVdF

Poly(vinylidene Fluoride) (PVdF) (CAS Number: 24937-79-9, Average Molecular Weight: ~530,000, pellets) (Sigma Aldrich) was used as polymer host of the gel polymer electrolytes. Chemical structure of PVdF is shown in Figure 2.1. The strong electron-withdrawing functional groups (-C-F-) could induce a net dipole moment [1]. Also, its high dielectric

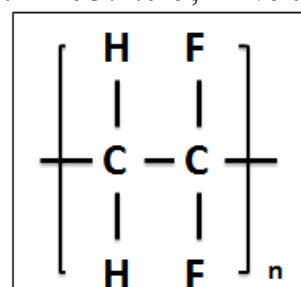


Figure 2.1 Chemical structure of PVdF

constant ($\epsilon = 8.4$) supports high concentration of charge carriers. Due to those excellent properties, PVdF was used as the major polymer host for the lithium ion polymer batteries studied in this work.

NMP

1-Methyl-2-pyrrolidone (NMP) (CAS Number: 872-50-4, Molecular Weight: 99.13) (Sigma Aldrich) was used as the solvent for PVdF because of its excellent virtue including non-toxicity, high boiling point (202°C - 204°C), low viscosity, low volatility, and high solubility. Chemical structure is shown in Figure 2.2.

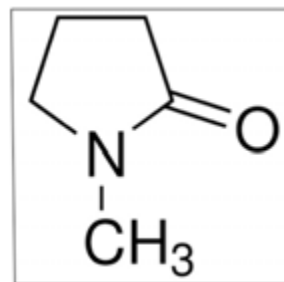


Figure 2.2 Chemical structure of NMP

LiPF₆

Lithium hexafluorophosphate (LiPF₆) (CAS Number: 21324-40-3, Molecular Weight: 151.91) (Sigma Aldrich) was the core material in electrolytes for lithium ion batteries, which transmitted lithium ions and electrons for anode and cathode. Based on the low associating ability of anions (PF₆⁻), LiPF₆ has high ionic conductivity that could enhance the electrolytes' ability of transmitting lithium ions and electrons.

EC & PC

Ethylene carbonate (EC) (CAS Number: 96-49-1, Molecular Weight: 88.06) (Sigma Aldrich) and propylene carbonate (PC) (CAS Number: 108-32-7, Molecular

Weight: 102.09) (Sigma Aldrich) was the plasticizer for PVdF membrane and the solvent for LiPF_6 . Chemical structures are shown in Figure 2.3. The cyclic carbonates, PC and EC, have high dielectric constant ($\epsilon(\text{EC at } 40^\circ\text{C})=89.78$ and $\epsilon(\text{PC at } 25^\circ\text{C})=64.92$), which is a significant advantage for dissolution of lithium salt; and, high flash point ($\text{FP}(\text{EC})=150^\circ\text{C}$ and $\text{FP}(\text{PC})=132^\circ\text{C}$), which is an important factor considering the safety[2].

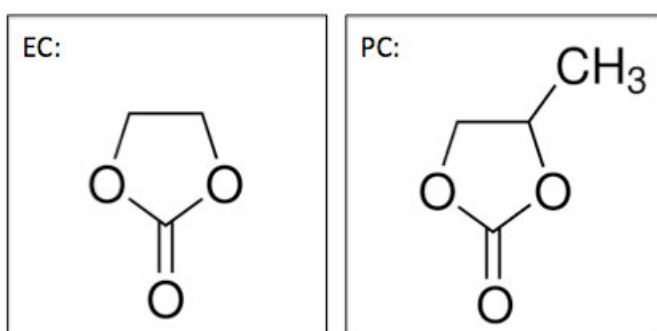


Figure 2.3 Chemical Structure of EC (left) and PC

EMI-TF

1-Ethyl-3-methylimidazolium

trifluoromethanesulfonate (EMI-TF) (CAS Number: 145022-44-2, Molecular Weight: 260.23) (Sigma Aldrich) was used as solvent for LiPF_6 . The molecular formula of EMI-TF is $\text{C}_7\text{H}_{11}\text{F}_3\text{N}_2\text{O}_3\text{S}$ and the chemical structure is shown in Figure 2.4. Chapter 3 discussed the influences of the concentration of EMI-TF as the solvent for LiPF_6 for lithium ion polymer batteries.

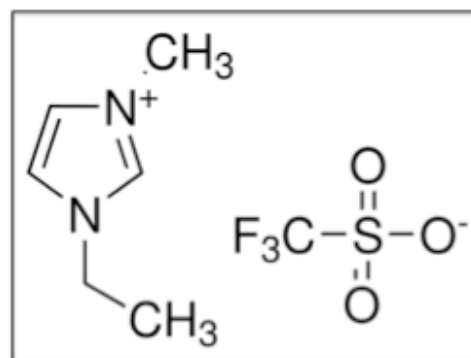


Figure 2.4 Chemical Structure of EMI-TF

AuNPs

Gold nanoparticles (AuNPs) were purchased from Purest Colloids, Inc. AuNPs dispersed in DI water with concentration of 20ppm and has average diameter 3.2nm. These AuNPs are functionalized with negatively charged functional groups and have Zeta potential of \sim -40mV. Since the PVdF-based GPE system is water sensitive, the water from AuNP solution was replaced with NMP through an solvent exchange process (Figure 2.5), before use as the additive in GPE system.

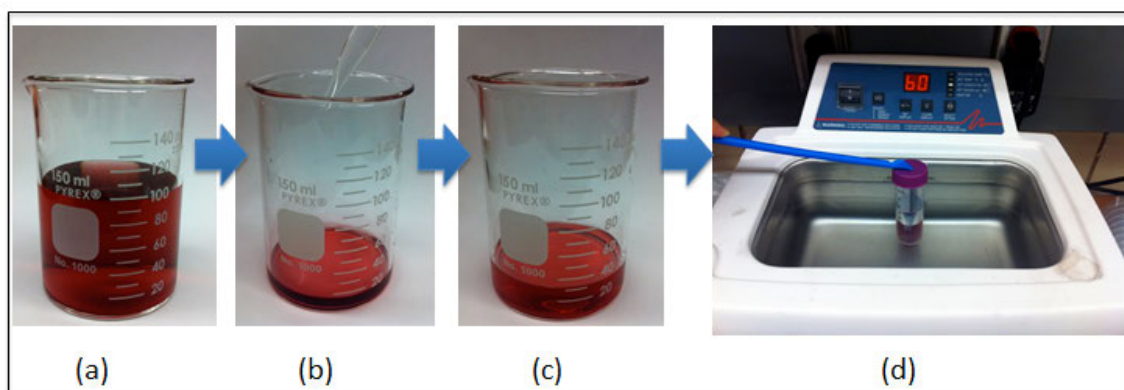


Figure 2.5 Solvent exchange for AuNPs solutions. a) 100mL AuNPs in DI water b) 5mL AuNPs in DI water after evaporating and adding new solvent of NMP c) AuNPs in 5mL DI water and 20mL NMP d) ultrasonic 20mL AuNPs in NMP after evaporating 5 mL water

Firstly, a 100mL of 20ppm AuNPs solution was located placed in the vacuum oven (-0.06MPa) under 90°C for 6 hours until the whole solution evaporated to 5mL. Then, 20mL NMP has been mixed as new solvent in the AuNPs solution. The new AuNPs solution with water and NMP as co-solvent was heated under vacuum to continue evaporate the solvent down to the volume of entire solution reached 20mL. Since the boiling point of NMP (202°C - 204°C) is much higher than the boiling point that of H₂O (100°C), the last 5mL solvent that has been evaporated was is assumed to be

water; and NMP was the only solvent left in AuNPs solution. In order to avoid prevent aggregation between of each AuNPs in NMP, the new 20mL AuNPs solution was placed under ultrasonicated for 1 hour. Finally, the AuNPs-NMP solution dispersion with concentration of 100ppm would was used in PVdF-based GPE system (section 2.2.2).

Anode and Cathode

Copper foil single-side coated by 0.1mm of Composite Graphite anode and aluminum foil single side coated by 0.1mm of lithium manganese oxide (LiMn_2O_4) cathode was purchased from MTI Corporation and used as received. The anode material of Graphite was casted on the surface of copper foil as the current collector; the cathode material of LiMn_2O_4 was casted on the surface of aluminum foil as the current collector (Figure 2.6). The coated foils were cut in $20\text{mm} \times 20\text{mm}$ pieces and used as the anode and cathode in assembly the lithium ion polymer battery package.

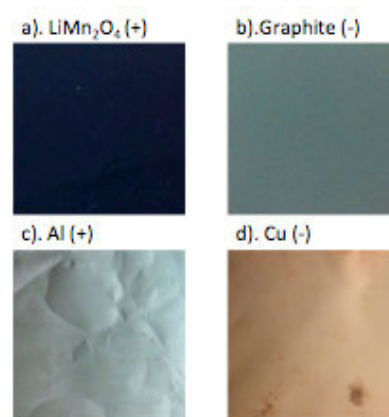


Figure 2.6 Composite Graphite anode and (LiMn_2O_4) cathode. a) the surface of LiMn_2O_4 on cathode; b) the surface of Graphite on anode; c) the surface of aluminum on cathode; d) the surface of copper on anode

2.2 Synthesis and activation

2.2.1 Gel Polymer Electrolytes with ionic liquids

Synthesis:

The membrane (Figure 2.7) was synthesized by first preparing a carbonate ester mixture. A 1:1 weight ratio mixture of EC and PC was heated to 80°C to achieve complete dissolution. The resultant clear carbonate ester solution (40%, weight percent) was mixed with PVdF (16%, weight percent) and 1-Methyl-2-pyrrolidone (44%, weight percent). The mixture was then heated to 110°C and stirred on magnetic stirrer until a clear solution was obtained with a relatively high viscosity. The solution was then casted on a glass template and left in vacuum oven under -0.08MPa at 80°C for 2 hours to form membranes. The membranes were then soaked in a 10% ethanol aqueous solution overnight. Pale yellow membranes with thickness of 50μm were obtained and cut into 20mm x 22mm squares and stored under ambient conditions.

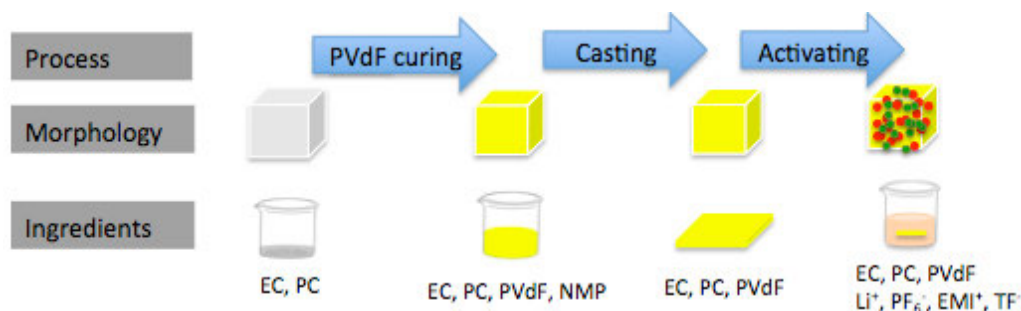


Figure 2.7 GPE fabricate process with ionic liquid (red dots present cations, and green dots present anions)

Activation:

The activation of the synthesized membranes was conducted by soaking them in organic electrolyte solution (LiPF₆ - EC - PC - EMI-Tf) for 24 hours. In order to narrow down the range of volume percentage of ILs (EMI-Tf) in the solvent, the activation part was separated into 2 steps. At the first step, to observe the effect of the ionic liquid on the GPE membrane we prepared five groups of samples containing EMI-Tf at different ratios from 0% to 100%, at 25% increments. According to the results from the first step that the lithium ion polymer batteries have better performance in the range of 25% EMI-Tf to 75% EMI-Tf, the volume percent of EMI-Tf in the second step was adjusted to 30%, 40%, 50%, and 60% for each group. For each group in step 1 and step 2, the concentration of organic electrolyte solution (LiPF₆) was kept constant at 1M.

Table 2.1 Solvent in volume percent of each group

Sample	1	2	3	4	5	6	7	8
EMI-Tf	0%	25%	30%	40%	50%	60%	75%	100%
EC	50%	37.5%	35%	30%	25%	20%	12.5%	0%
PC	50%	37.5%	35%	30%	25%	20%	12.5%	0%

2.2.2 Gel Polymer Electrolytes with nanomaterials

As presented in Figure 2.8, the GPE is a membrane synthesized by trapping plasticizers EC and PC in PVdF and NMP solution. Firstly, EC and PC with weight ratio of 1:1 were mixed and heated at 110°C to completely dissolve. Then, PVdF was added to pure NMP at 4:11 weight ratio as the control group; and PVdF added to 100ppm AuNPs-NMP solution with the same weight ratio as the experimental group. Then the EC-PC solution was mixed with the control and experimental group at 2:3 ratio. The two

resultant solutions were heated at 110°C and stirred on a magnetic stirrer until desired viscosity was reached. The slurry was then casted onto a flat glass disk. The flat glass disk with the slurry was then left in vacuum oven under -0.08MPa at 80°C for 2 hours; and then soaked in 10% ethanol solution for 12 hours. Next, a pale yellow membrane for the control group and a light purple AuNPs-doped membrane for the experimental group were remained in the glass disk. The membranes in both groups had thickness of 0.3mm and were cut into 22mm × 22mm square and were stored at ambient conditions. The activation of the synthesized membranes was conducted by soaking them in a 1M solution of LiPF₆ – EC & PC (1:1) for 24 hours.

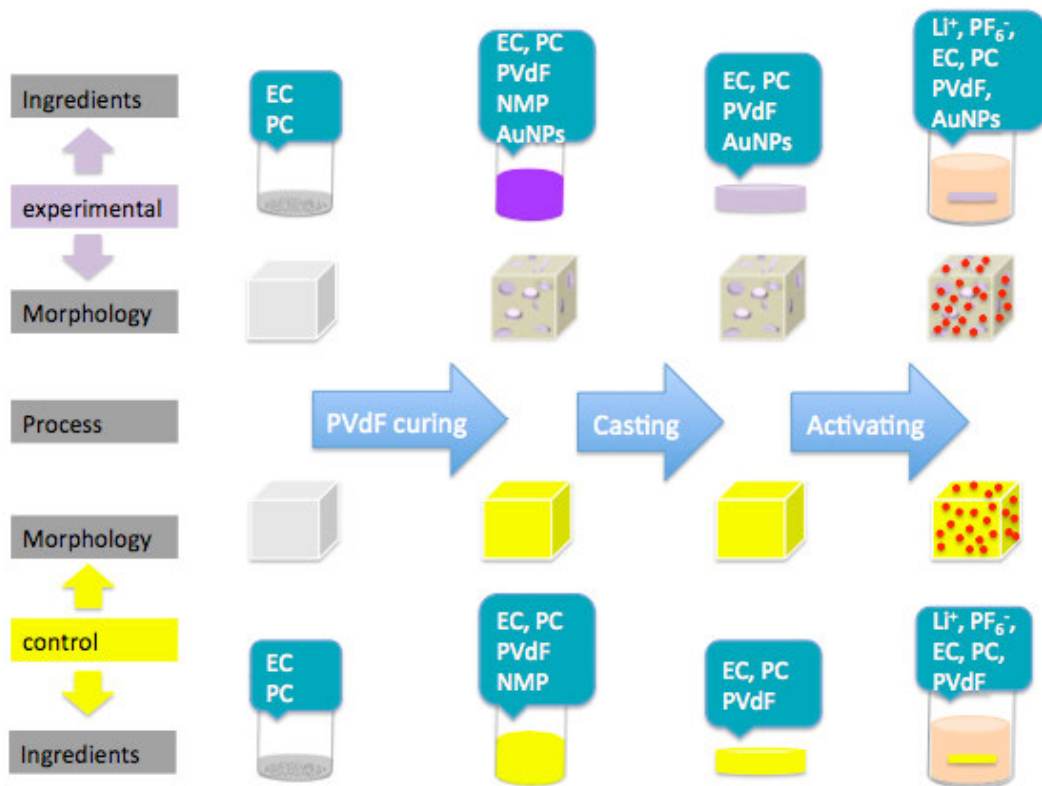


Figure 2.8 GPE fabricate process with AuNPs (red dots present Lithium ions, and purple dots present AuNPs)

2.3 Lithium ion Polymer Battery Assembly

The thin-film cell was assembled as shown in Figure 2.9; with GPE located in between the cathode and anode. In the actual model on the left of Figure 2.9, cathode and anode are exactly $20\text{mm} \times 2\text{mm}$; but GPE film is larger than cathode and anode so the cell would not be shorted. The surface of protection cover that faces inside of the cell is adhesive, which helped airtight enclosure of the whole system.

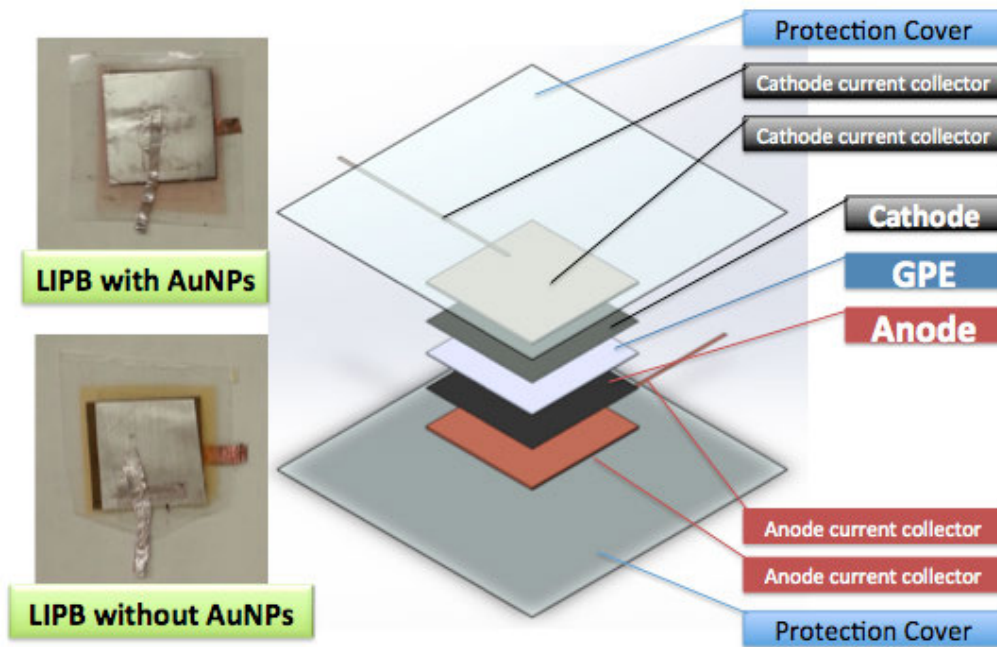


Figure 2.9 Structure of LIPB. Insets on the left show photographic images of the actual structure

2.4 Measurements

2.3.1 VersaSTAT-4

A VersaSTAT-4 potentiostat (Princeton Applied Research) (Figure 2.10) was used for



Figure 2.10 VersaSTAT 4 www.manaraa.com

electrochemical and impedance spectroscopy studies of the gel polymer electrolyte.

Ionic Conductivity:

The ionic conductivity of GPE was measured by impedance spectroscopy using two steel chips (15.5mm D × 0.2mm T) as the blocking electrode cells. The GPE membrane was placed between two steel chips; and an enclosing case (Figure 2.11). The detailed drawing of the enclosing case is presented in the Appendix.

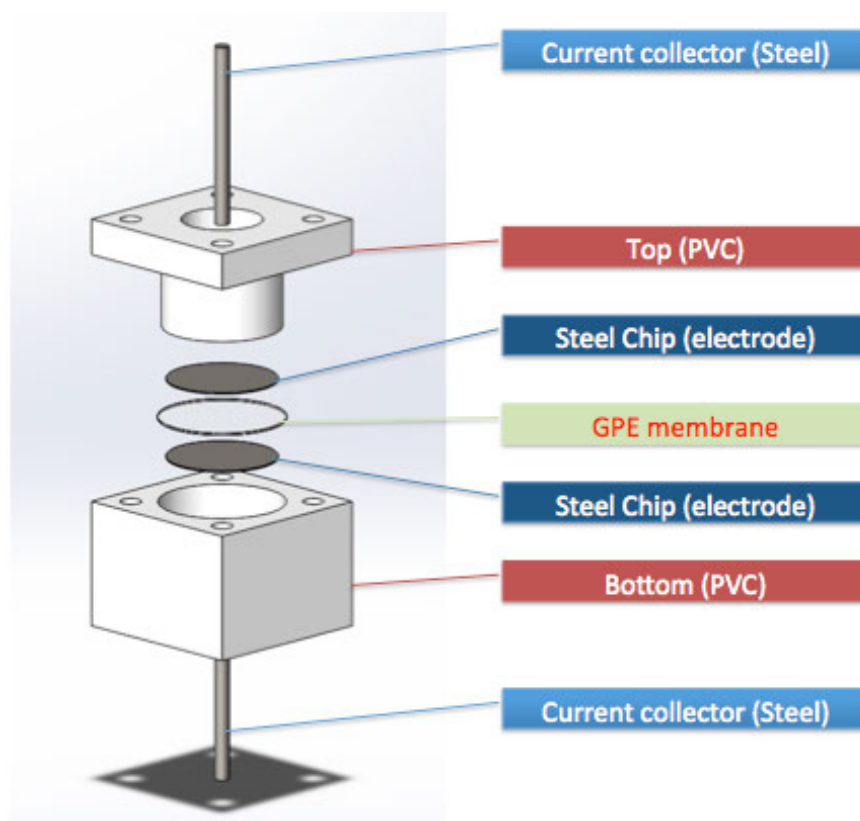


Figure 2.11 Ionic Conductivity testing cell

The impedance spectroscopy studies (Figure 2.12) were carried at frequency range of 1.0E5Hz to 0.1Hz and potential difference (ΔV) of 10mV.

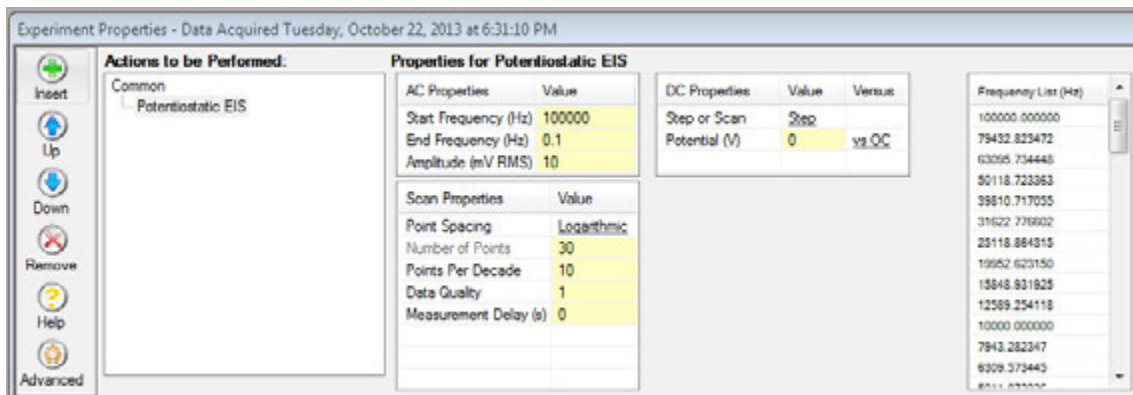


Figure 2.12 Setup of impedance spectroscopy

Interfacial properties:

The interfacial properties of GPE were measured by impedance spectroscopy with thin-film cell after finishing 10 cycles charging and discharging, which was assembled as shown in Figure 2.9. The impedance spectroscopy studies were also carried at frequency range of 1.0E5Hz to 0.1Hz and potential difference (ΔV) of 10mV, same as the setup for ion conductivity measurement. For the experiments involving GPE doped with AuNPs, the impedance of the thin-film LIPB (both control group and experimental group) was periodically monitored over 30 days, in order to compare the reliability of the batteries. In Chapter 4 we discuss the details of the measurement after 1 day, 4 days, 7 days, 15 days, and 30 days.

2.3.2 Ultraviolet

The AuNPs were characterized by Ultraviolet-Visible spectrometer



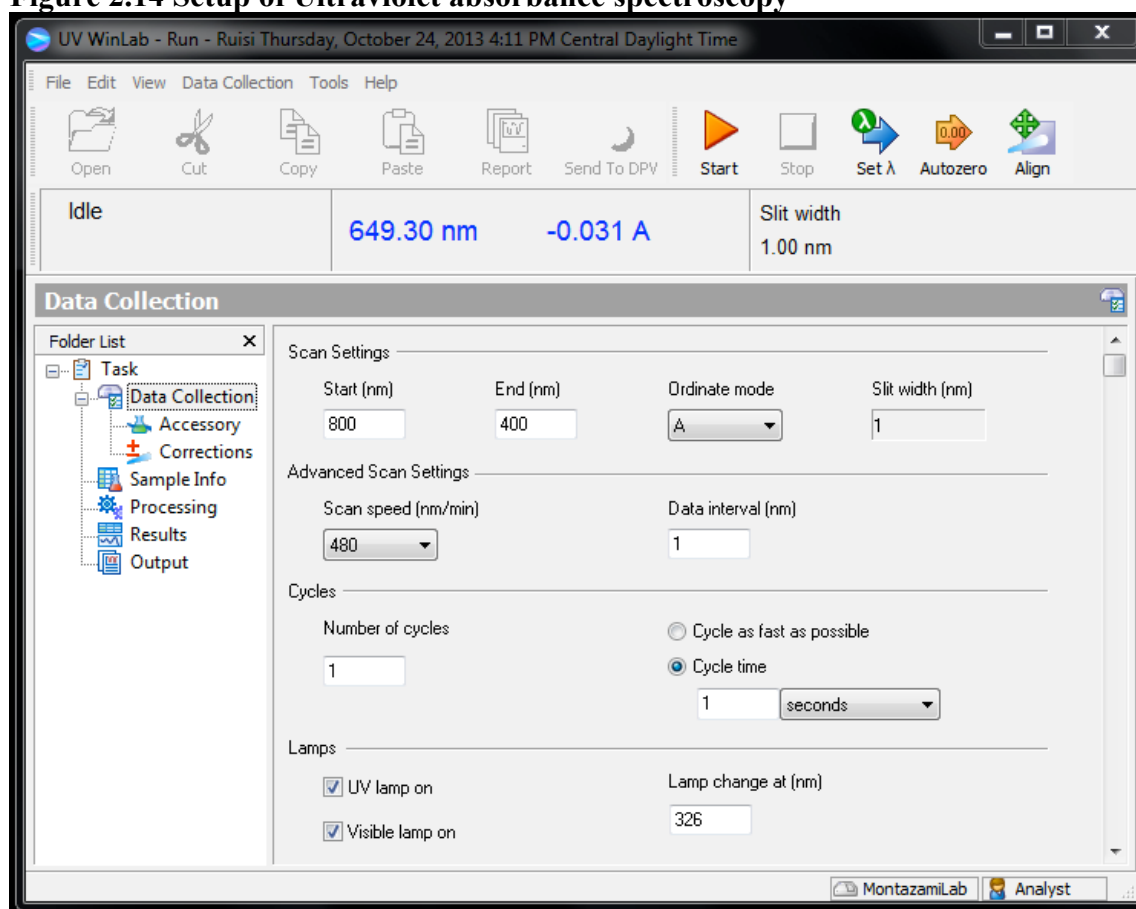
Figure 2.13 PerkinElmer Ultraviolet spectrometer

(PerkinElmer) (Figure 2.13). The Ultraviolet absorbance tests were conducted three times in the entire solvent exchange process, which is listed below.

1. The original AuNPs solution with medium of DI water before solvent exchange
2. The 5mL AuNPs solution with medium of DI water after evaporation and before adding NMP
3. The final 20mL AuNPs solution with medium of NMP after sonication.

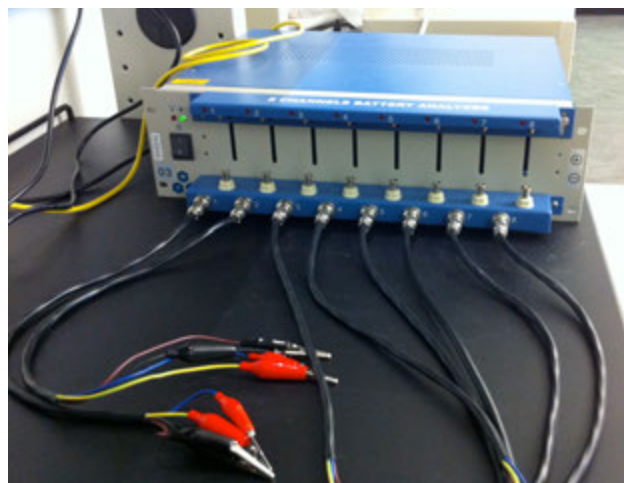
Ultraviolet spectrum (Figure 2.14) scanned the sample from 800nm to 400nm with scan speed of 480 nm/min. Before running the test, the base line was obtained with DI water filled cuvettes.

Figure 2.14 Setup of Ultraviolet absorbance spectroscopy



2.3.3 BST8-MA battery analyzer

Charge-discharge tests were carried out with a computer controlled BST8-MA battery analyzer (MTI corporation), between 1.5V and 4.2V with a constant current of 0.5mA. Battery analyzer was able to charge



the battery with constant current or constant voltage, and discharge the battery with constant current or constant voltage. Meanwhile, this equipment also monitored the capacities, current and voltage of the batteries as a function of time. As shown in Figure 2.16, battery tests started with a constant discharge current of 0.5mA until the voltage decreased to 1.5V. After the system paused for 2 minutes, it started charging the battery with a constant current of 0.5mA and then constant voltage of 4.2V. A complete charging-discharging process called a cycle. Every lithium ion polymer battery was tested for 51 cycles total.

Figure 2.15 BST8-MA Battery Analyzer

Step Set

Step No	Step Name	Time(min)	Voltage(V)	Current(...)	Capacity(...)	-dV(mV)	Power(...)	Resista...	Jump...	Cycles	CurrStop(mA)
1	C_Curr Disc...		1.5000	0.500							
2	Rest	2									
3	C_Curr Charge		-4.2	0.5							
4	C_Volt Charge		-4.2	2							
5	Rest	5									
6	Cycle								1	50	
7	End										

From 1 Startup

Delay Prot: 0 Sec. CapPerVal: mg

Record condition

Time: 1 Sec.
 Current: 0 mA
 Voltage: 0 mV

Protect Param

Hi Voltage: 5 V
 Low Voltage: 0 V
 Current Range 0 mA

Base Information

Creator:
Batch No:
Memo:

Back Setting
NDB Setting

Clear Step Save File Open File OK Cancel

Figure 2.16 Setup of BST8-MA Battery Analyzer

REFERENCES

- [1] D. M. Esterly, "Manufacturing of Poly (vinylidene fluoride) and Evaluation of its Mechanical Properties," 2002.
- [2] T. Tamura, K. Yoshida, T. Hachida, M. Tsuchiya, M. Nakamura, Y. Kazue, N. Tachikawa, K. Dokko, and M. Watanabe, "Physicochemical properties of glyme–Li salt complexes as a new family of room-temperature ionic liquids," *Chemistry Letters*, vol. 39, pp. 753-755, 2010.

CHAPTER 3

INFLUENCE OF IONIC LIQUIDS OF THE GEL POLYMER ELECTROLYTE

3.1 Introduction

In the recent years application of Li-ion batteries in common electronic devices, and thus demand for more efficient and safer batteries, has increased significantly [1-4]. Batteries with higher efficiency, superior mechanical properties and smaller size [5] are needed for handheld electronics to keep up with the rapidly increasing computing power, larger screens and thinner and lighter designs of such devices. There has also been a significant increase in concerns regarding the issues associated with such batteries. Use of flammable organic solvents as electrolyte, formation of lithium dendrites, and large volume change due to poor structural stability are among the main concerns associated with Li-ion batteries. Use of gel polymer electrolytes has addressed some concerns regarding leakage of liquid electrolytes and the resultant fire hazards; however, charge transfer through GPE doped with organic solvents is not as efficient as that in liquid electrolytes. Also, doping GPE with organic solvents poses some limiting difficulties.

Generally, synthesis of GPEs is achieved by incorporating an organic electrolyte solution into a polymer matrix with a trapping structure enhanced by carbonate esters [6, 7]. Polymer matrices with high chemical stability and strong electron-withdrawing functional groups to induce a net dipole moment are desirable as the polymer host [8]. One polymer commonly used in gel polymer electrolytes is polyvinylidene fluoride (PVdF) (containing -C-F functional groups. The PVdF base gel polymer electrolyte

membranes attract ions in the organic electrolyte solution due to the electric field at the surface of the PVdF membrane, because of the semi-crystalline structure of PVdF part of the attracted ions are drafted into the membrane when the rest of ions stay at the surface[9-13]. Thus, a gel polymer electrolyte membrane with fully interconnected open microspores, i.e. higher interfacial surface area, enhances ion storage and mobility [11, 14-18].

Comparing to liquid electrolytes, GPEs have several advantages, such as superior mechanical properties, faster charging/discharging and higher power density [19-21]. However, ion permeability of GPEs is orders of magnitude lower than that of liquid electrolytes, mainly because of the polymeric structure which limits the ion mobility [8, 22].

Room temperature ionic liquids have been used to substitute organic electrolytes to increase ion mobility throughout the electrolyte and also to eliminate hazards associated with organic electrolytes. Application of ionic liquids in lithium-ion batteries has been focus of several studies in the recent years. Fernicaola *et al.*, incorporated ionic liquids in an organic electrolyte solution to increase the ionic conductivity and stabilize the lithium ions carried on the surface of PVdF-base membrane [23]. In one study Egashira *et al* have shown than the ion mobility through the gel electrolyte containing ionic liquids depends on the miscibility of polymer component in the ionic liquid. It was shown that, for example, gel electrolyte containing hexyltrimethylammonium bis(trifluoromethane sulfone)imide ionic liquid exhibit high lithium ion permeability whereas no obvious lithium ion mobility was detected through a gel electrolyte

contusing 1-ethyl-3-methyl imidazolium bis(trifluoromethane sulfone)imide ionic liquid [24]. In other studies it was demonstrated that the ion permeability of the gel electrolyte could be improved by addition of carbonate esters. Carbonate esters play the role of ion dissociation enhancer and improve ion mobility because of their relatively high dielectric constants. Ethylene carbonate ($\epsilon = 89.78 @ 40^{\circ}\text{C}$) and propylene carbonate ($\epsilon = 64.93 @ 25^{\circ}\text{C}$) are among the most common carbonate esters used in lithium-ion polymer batteries. They both have excellent thermal stability and boiling point of above 240°C [25]. Ye *et al* doped the gel electrolyte by a small amount of ethylene carbonate and observed a significant increase in lithium ion transport through the gel electrolyte [26]. Sirisopanaporn *et al* demonstrated higher ion permeability and interfacial stability by addition of small amounts of ethylene carbonate and propylene carbonate to the gel electrolyte [27]. A vapor-free lithium-ion polymer battery with high discharge performance based on lithium salt dissolved in ionic liquid and ultra-high molecular weight ionic liquid polymer was reported by Sato *et al*. it was demonstrated that the discharge performance is higher than that of a conventional lithium polymer battery [28].

In view of the progress of the technology, as well as the safety of the lithium ion battery technology, it is highly desired to further investigate polymer base electrolytes doped with ionic liquid induced electrolytes.

In this work we attempt to fill the gap between efficient systems base on organic solvents and safe and reliable systems base on ionic liquids. We have investigated gel polymer electrolytes doped with a mixture of organic electrolyte and ionic liquid at

different ratios, in presence of carbonate esters, to enhance ion permeability and electrochemical properties of the gel polymer electrolytes.

The traditional organic electrolyte solution of LIPBs is dissolving lithium salt into carbonate solvent solution [29-31]. In this case, Lithium Hexafluorophosphate (LiPF_6) is chosen as the lithium salt due to its high conductivity in carbonates solvent mixtures and the ability to prevent aluminum corrosion at the cathode aluminum current collector by forming a passivation layer. Also, cyclic carbonates mixture EC and PC (wt% 1:1) are considering as the solvent for LiPF_6 , which

Li et al found that the radius the complex ion solvent is smaller for the EC/PC mixture than either pure EC or pure PC, which will help dissolving lithium salts [32]. Among aprotic ILs, protic ILs, and Zwitter ILs, the aprotic class of ILs with high mobility and ion concentration stands out as advanced LIPB electrolytes, which consists of large irregular cations and small anions [33].

This work picks 1-ethyl-3-methylimidazolium trifluoromethane (EMI-TF) due to its high ionic conductivity (10^{-2} S/cm) and wide electrochemical window. The EMI cations' dangling alkyl groups and the planar imidazolium ring with the delocalization of charge over the N-C-N moiety serve to decrease ion-ion interactions and higher the mobility [34, 35]. This work discussed the effects of varies volume ratios of ILs to get the best improvement on Li-ion batteries.

3.2 Experimental

Materials:

Copper foil single-side coated by 0.1mm of Composite Graphite anode, aluminum foil single side coated by 0.1mm of lithium manganese oxide (LiMn_2O_4) cathode, lithium chips, and Super P (conductive carbon) were purchased from MTI corporation and used as received. N-Methyl-2-pyrrolidone (NMP), ethylene carbonate (EC), propylene carbonate (PC), lithium hexafluorophosphate (LiF_6PO_4), polyvinylidene fluoride (PVdF), and 1-Ethyl-3-methylimidazolium trifluoromethanesulfonate (EMI-TF) were purchased from Sigma-Aldrich and used as received.

Synthesis:

The membrane was synthesized by first preparing a carbonate ester mixture. A 1:1 weight ratio mixture of EC and PC was heated to 80°C to achieve complete dissolution. The resultant clear carbonate ester solution (40%) was mixed with PVdF (16%) and 1-Methyl-2-pyrrolidone (44%). The mixture was then heated to 110°C and stirred on magnetic stirrer until a clear solution was obtained with a relatively high viscosity. The solution was then casted on a glass template and left under -0.08MPa at 80°C for 2 hours to form membranes. The membranes were then soaked in a 10% ethanol aqueous solution overnight. Pale yellow membranes with $50\mu\text{m}$ thickness were stored under ambient conditions.

Activation:

The activation of the synthesized membranes was soaked them in organic electrolyte solution (1M LiPF_6 solvent) for 24 hours. To observe the effect of the ionic liquid on the

GPE membrane, we prepared eight group with different volume percent of EMI-Tf in the solvent: 0%, 25%, 30%, 40%, 50%, 60%, 75%, and 100%, and the rest solvent was EC and PC (1:1).

Measurements:

A VersaSTAT-4 potentiostat (Princeton Applied Research) was used for electrochemical and impedance spectroscopy studies of the gel polymer electrolyte membranes. For these studies GPE membranes were secured between two steel-disks electrodes of 200 μ m thickness and 15.5mm diameter, and two pieces of adhesive plastic were used as a pouch to seal and hold each sample. The electrochemical studies were carried out by cyclic voltammetry measurements at 10mV/s scan rate. The impedance spectroscopy studies were carried at frequency range of 1.0E5Hz to 0.1Hz and potential difference (ΔV) of 10mV, after completion of 10 charging/discharging cycles. In each sample, the membrane was cut slightly larger than the electrodes to prevent short-circuit. Charge-discharge tests were carried out with a computer controlled BST8-MA battery analyzer (MTI corporation), between 1V and 5V with a constant current of 0.5mA.

3.3 Results and discussion

3.3.1 Ionic Conductivity:

GPEs were studied for their ion permeability by AC impedance spectroscopy. GPEs doped with electrolytes of different EMI-Tf/EC/PC ratios were secured between steel disks and studied at a high frequency range (10000Hz – 100000Hz). As presented in Figure 3.1, the Nyquist plot exhibited approximately vertical lines, suggesting nearly

pure resistive behavior at high frequencies, for all GPE samples. Here, the effect of imaginary part of the impedance can be neglected and the system can be considered as a pure resistor with minimum dependence on frequency. The internal resistance of the bulk electrolyte can be induced from the intercept of the extended impedance plots with the x-axis (Z_{re}). Electrical conductivity of GPEs can be calculated using internal resistance, thickness and cross-section area of the GPEs. . The electrical conductivity σ for each GPE sample was calculated using Equation 1:

$$\sigma = \frac{t}{RA} \quad (1)$$

were t is the thickness of each sample, R is the internal resistance and A is cross section area (1.89 cm^2). Ionic permeability of GPE samples is presented in Table 1.

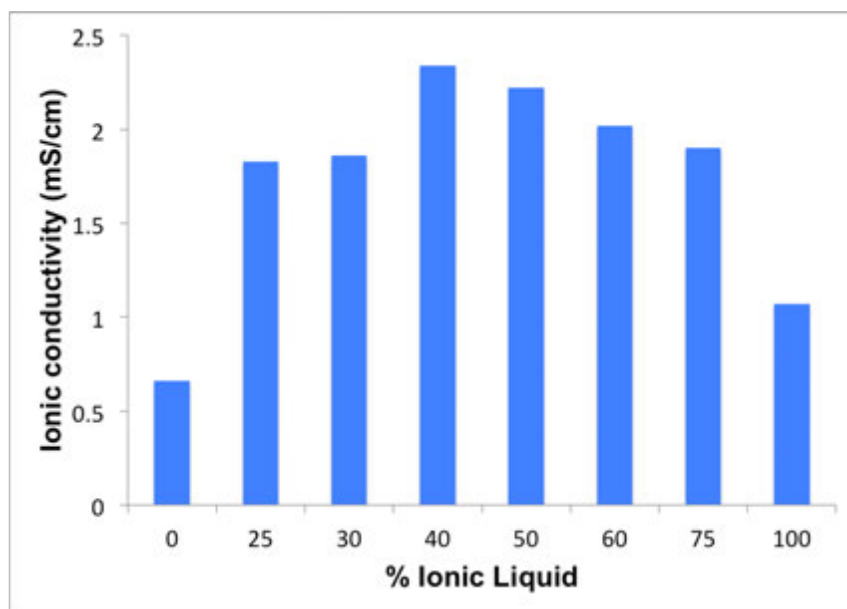


Figure 3.1 Bar chart of Ionic conductivity

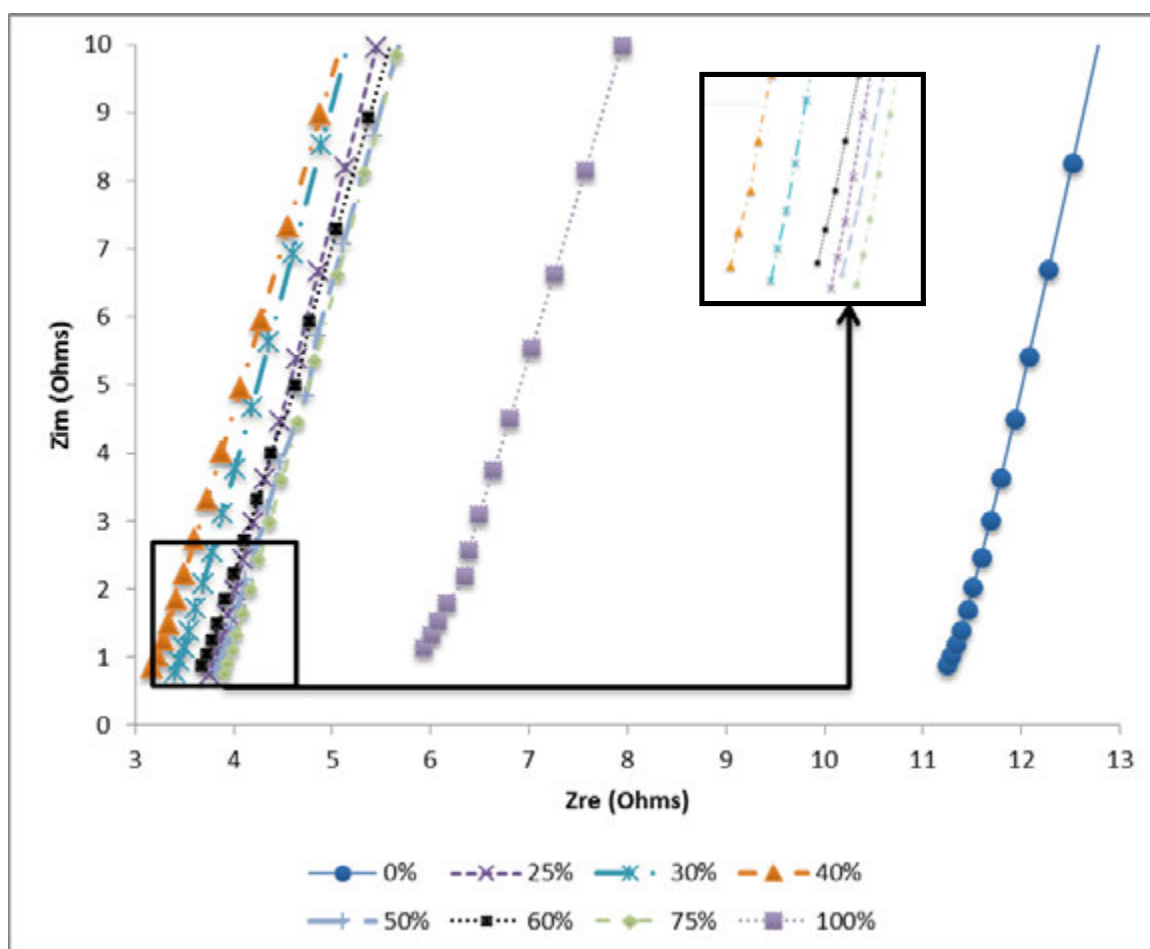


Figure 3.2 Nyquist plots of steel/GPE/steel with different volume percent ionic liquids at high frequency

Table 3.1 Values of each term in calculating ionic conductivity

Cross area (cm ²)	Percent of ILs (%)	Internal resistance (Ohms)	Thickness (cm)	Electrical conductivity (mS/cm)
1.89	0	11.2379	0.014	0.66
	25	3.7595	0.013	1.83
	30	3.4118	0.012	1.86
	40	3.1770	0.014	2.34
	50	3.8264	0.016	2.22
	60	3.6806	0.014	2.02
	75	3.9111	0.014	1.90
	100	5.9292	0.012	1.07

Samples containing EMI-Tf ionic liquid exhibited ~65% to ~250% improvement on their ion permeability compare to sample without EMI-TF (100% EC-PC solvent). Interestingly, ionic permeability of the GPEs showed an increasing trend as the ionic liquid content increased to ~40% and decreased thereafter, suggesting the significant contribution of EC and PC to ion permeability of the GPEs. It is important to note that the measured ionic permeability in this study is due to the movement of all ions in the PVdF-based electrolyte, including Li^+ , EMI^+ , TF^- , and PF_6^- (EMI^+ and Tf^- only when ionic liquid was used). Previous studies[17, 36-38] have shown that compare to diffusions among cations, the EMI^+ always diffuses faster than smaller Li^+ , and that Li^+ and anions are more likely to form ion complexes and diffuse together at a slower rate. High electrical conductivity of EMI-Tf (6.4 mS/cm) at room temperature contributes significantly to the ion permeability of the GPE membrane [32, 39]. Yet, GPE's containing EMI-Tf as the only solvent exhibited relatively low electrical conductivity, comparable to that of samples containing EC-PC solvent only. The importance and effect of EC and PC should not be neglected, which enhanced to improve the Li ion transport and dissociate the Li ion complexes due to their excellent physic-chemical properties, such as high dielectric constant and good thermal stability [26]. Although the ionic conductivity of GPE with variances of concentration of ILs seems the similar (~2 mS/cm), at the first glance, there existed an order of ionic conductivities from high to low, which is 40 v% ILs, 50 v%, 60 v%, 75 v%, 30 v% and 25 v%. Seeking the balance between EC, PC and EMITF, based on the experimental results the electrolytes containing 40 v% ~ 50 v% had the most efficient diffusion among Li^+ , EMI^+ , TF^- , and

PF₆⁻. 40 v% ~ 50 v% provided free EMI cations to enhance the ionic conductivity; and 60 v% ~50 v% EC and PC solution decomposed Li ion complexes and freed Li ions that were relevant for the charge/discharge of LIPBs.

3.3.2 Interfacial properties:

The interfacial properties of GPE were monitored by impedance spectroscopy (1.0E5 Hz to 0.1 Hz, $\Delta V=10\text{mV}$) as thin-film cell pack after finishing 10 cycles charging and discharging. The curves of Nyquist Plots for all cells were consist of semicircles and followed by an approximately linear plot (Figure 3.3).

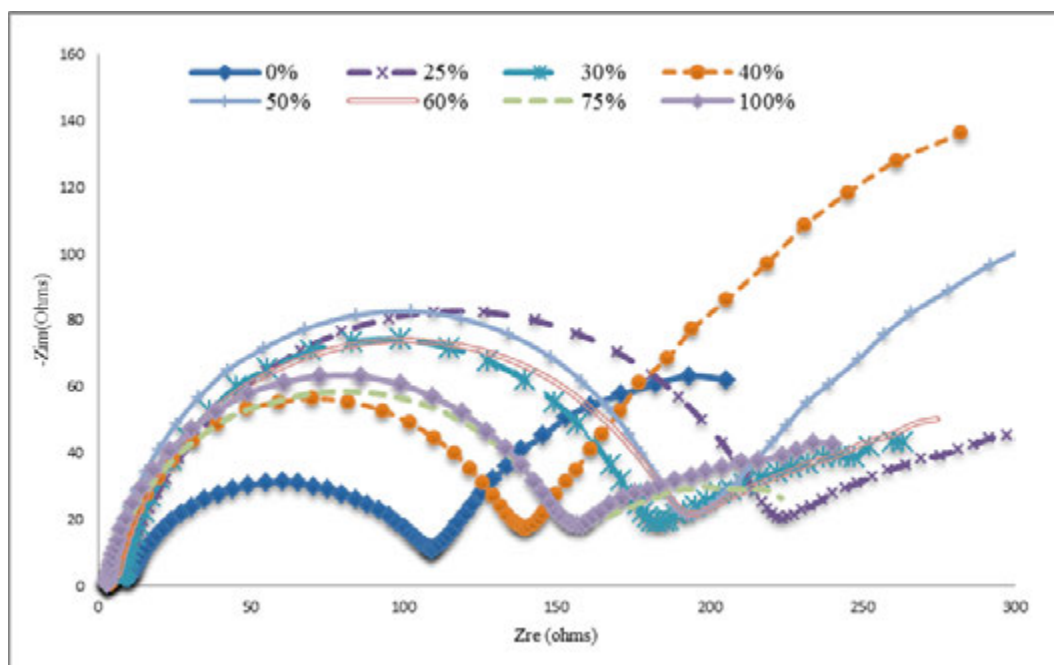


Figure 3.3 Nyquist plots of Graphite/GPE/LiMn₂O₄ with different volume percent ionic liquids

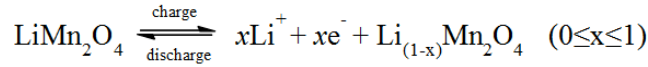
At high frequencies, the start points of semicircles, the battery system could be considered as “pure resistor” since it was almost a vertical line. Extending the vertical

line until intersecting the x-axis, the impedance at the intersection represents the value of “pure resistor”, called the solution resistance (R_s) in the equivalent circuit. Solution resistance depends on the ionic conductivity of the entire system including the transportation of ions between anode and cathode; so it would be slightly distinct with the ionic conductivity discussed in the previous section. However, according to the value in Figure 3.3, second to the 100 v% ILs that exhibited smallest solution resistance (i.e. highest ionic conductivity), the solution resistance of GPEs with 40 v% ~ 50 v% ILs was the smallest among GPEs with mixed electrolyte.

Assuming the semicircles are associated with the parallel combination of charge transfer resistance (R_{CT}), and double layer capacitance (C_{DL}), and Warburg impedance (W) in series, the system could be described as the equivalent circuit in 3.4 [40, 41]. The charge transfer resistance is known as the diameter of the semicircle, which could be measured by the real impedance difference between the right end point of the semicircle and the left start point. When the entire system at equilibrium, the overpotential was very small, Equation 2 could be used to define charge transfer resistance (Figure 3.3) that is known from the Nyquist plot [42]. I_0 (exchange current density), representing the speed of charge transfer reaction, was the only factor that depended on charge transfer resistance, since others, R (gas constant), T (temperature), n (number of electrons involved), and F (Faradays constant), were constant. In this work, LiMn_2O_4 was the cathode that dissolved the Li ions into the GPE, according to the following reaction [43, 44]. However, GPEs with ILs increased the charge transfer resistance, which means they

decreased the speed of reaction, because the protons at C-2 position of imidazolium cations constrained the chemical reduction [23].

$$R_{CT} = \frac{RT}{nFi_0} \quad (2)$$



At the middle of the semicircle, the impedance was almost capacitive contribution due to the derivative of the curve at this point was nearly zero, so the imaginary impedance and the frequency at this point could be used for calculating the double layer capacitance (Equation 3) [45, 46]. Also, with the content of ionic liquids increasing, the double-layer capacitance (C_{DL}) increased except at 25%. With more ionic liquid, the cell was able to contain more ions (smaller solution resistance) and store more energy (larger double-layer capacitance). However, there existed exceptions around 25 v% of ILs with high solution resistance and low double-layer capacitance. In small amount of ionic liquid, the organic electrolyte solution was not stable and the ability of ions from ILs attaching on GPE membranes is low compare with higher percentages of ILs. The battery system preferred higher percentages of ionic liquids.

$$C_{DL} = \frac{2\pi}{f_m Z_{im,m}} \quad (3)$$

The linear plot associated with the semicircle at low frequency, called low frequency Warburg line, represented the Warburg behaviors - diffusion between two electrodes. Based on the experiment results, the Warburg behaviors could be obtained by the Warburg coefficient (σ_s): the slope of the line real impedance verses the radial

frequency to the power of (-1/2) (Figure 3.5). Theoretically, σ_s could also be defined by Equation 4, where R is the gas constant, T is the room temperature in this experiment, n is the number of electrons transferred, F is the Faradays constant, A is the surface area of the electrode, C_O^* is the bulk concentration of the diffusing species from oxidant, D_O is the diffusion coefficient of the oxidant, C_R^* is the bulk concentration of the diffusing species from reductant, and D_R is the diffusion coefficient of reductant. Based on the equation 4, the Warburg behaviors were more relayed on diffusing properties of the reductant and the oxidant, which are the two electrodes, and GPE has few effects on the diffusions. It also proved by the number of Warburg coefficients of those 8 groups, since there were no certain patterns overall among them.

$$\sigma = \frac{RT}{n^2 F^2 A \sqrt{2}} \left(\frac{1}{C_O^* \sqrt{D_O}} + \frac{1}{C_R^* \sqrt{D_R}} \right) \quad (4)$$

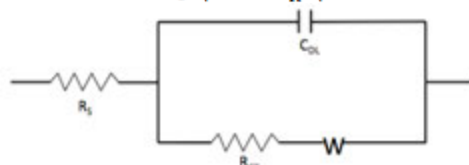


Figure 3.4 Equivalent circuit of Lithium-ion polymer cell

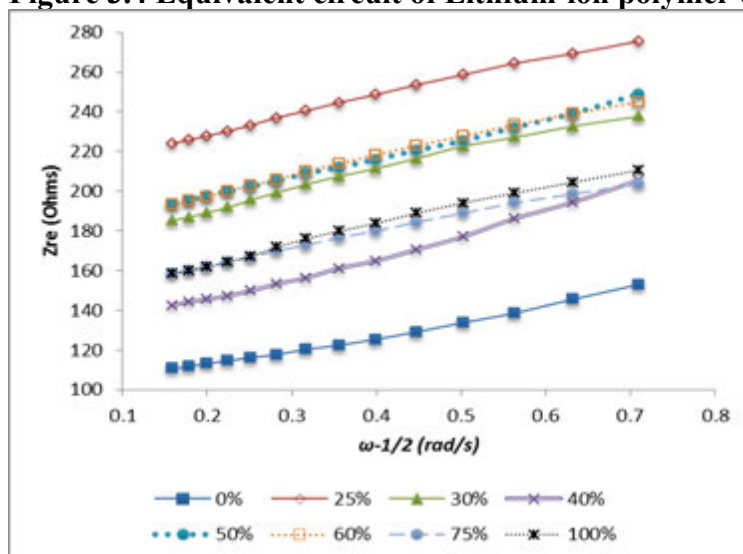


Figure 3.5 Real impedance versus the radial frequency to the power of (-1/2) at low frequency (63 Hz ~ 3 Hz)

Table 3.2 Values of solution resistance and double-layer capacitance in equivalent circuit

Percent of ILs (v%)	R _s (Ohms)	R _{CT} (Ohms)	C _{DL} (F)	τ_s
0	9.983	98.940	3.99E-04	78.814
25	7.475	216.578	3.03E-04	95.976
30	5.517	177.381	4.25E-04	99.088
40	3.785	136.122	4.43E-04	113.52
50	2.849	190.677	4.80E-04	97.602
60	3.968	189.382	4.43E-04	95.877
75	3.065	155.311	5.36E-04	84.32
100	2.931	154.235	6.54E-04	98.015

3.3.3 Battery performance:

Galvan static charging and discharging were used to evaluate to performance of the entire system (Graphite/GPE/LiMn2O4). Each cycle included constant current (0.5C) discharging, rest (8mins), constant current charging and constant voltage charging in the voltage range of 0.5V – 5V. During each process, the Battery Analyzer monitored the current, voltage, and capacities every 5 seconds.

The battery performance could be represented by the value of discharge capacity along shelf life and average rest voltages after fully charged. Table 3.3 displayed the average rest voltage (RV) of each system after fully charged; RV(50v%)>RV(30v%)>RV(40v%)>RV(25v%)>RV(60v%)>RV(0v%)>RV(75v%)>RV(100v%).

Figure 3.6 compared the cycling stability of each battery system. At the first 25 cycles (Figure 3.6), systems with ionic liquid had much higher discharge capacity (~90mAh/g) comparing with the system without ionic liquid (~80mAh/g). At the last 25 cycles, the discharge capacity of system with 75 v% and 100 v% ILs decline rapidly

from 90mAh/g to 50mAh/g; and almost 55 v% of discharge capacity lost in the last 25 cycles comparing with the initial discharge capacity. Low average rest voltage and high discharge capacity lost indicated that the systems with high volume percent of ionic liquids were not stable at long terms due to the acidic proton in C-2 on the EMI cations would damage the protective film on the surface of electrodes [21]. As the protective film is damaging, there would be a series of side reactions occurred between GPE and the electrodes. In this case that LiPF_6 was the main solute; it was highly possible that CO_2 , HF, and LiF would be produced by side reaction. Gas CO_2 and HF gases would increase the internal pressure of the cell, which would cause safety concerns and even lead to explosion. LiF was not in ionic form and barely electrical conductive leading to high interface resistance. Other than 75 v% and 100 v%, GPEs, with ILs 0 v%, 25 v%, 30 v%, 40 v% 50 v% and 60 v%, kept discharge capacity in less than 20% of the initial value (Figure 3.6). Overall, the discharge capacity of GPEs increased as the volume percent of ILs increasing from 0 v% to 50 v%; however, it declined after 50 v%. GPEs with ILs 50 v% reached the peak of discharge capacity. Based on the data in Figure 3.6, at ILs 50 v%, there was a balance between ILs and mixture of EC and PC. According to Hui et al, ethylene carbonate could form an effective protective layer on the surface of graphite as a co-solvent to prevent side reactions [39]. PC and EC were both cyclic carbonate; and they enhanced the stability and transport of lithium ions as PC and EC mixture. In this case, half volume of the solvent – EC and PC mixture - provided the protective film; and the other half - Ionic Liquids – increased the ionic conductivity of GPEs.

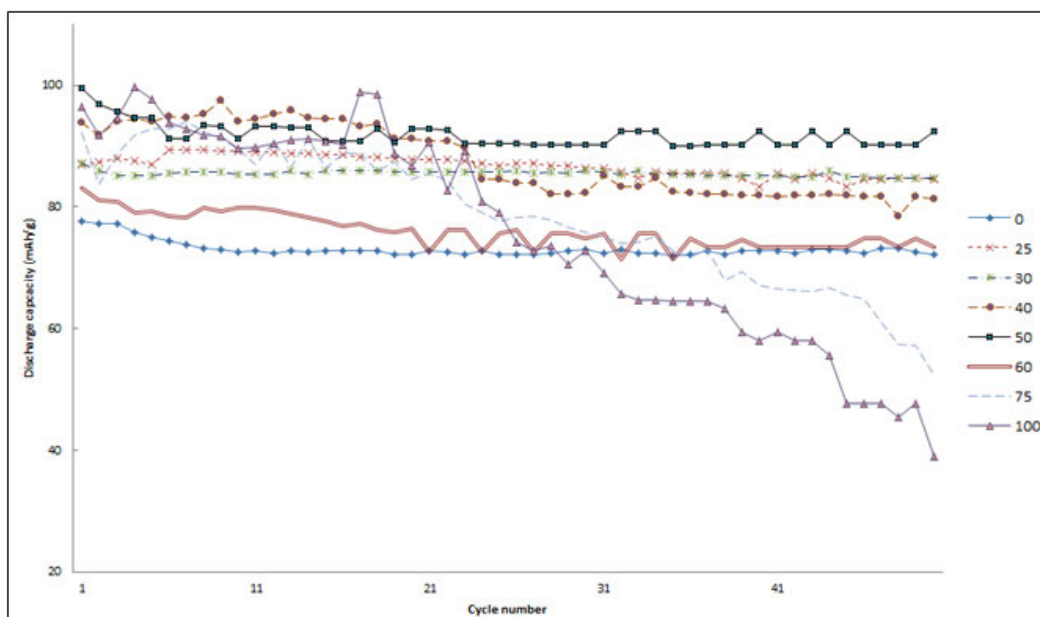


Figure 3.6 Consecutive cycling behavior of Graphite/GPE/LiMn₂O₄ systems with different volume percent of ionic liquids

Table 3.3 The average rest voltages of Graphite/GPE/LiMn₂O₄ systems with different volume percent of ionic liquids after fully charged

Volume percent of ILs (v%)	Rest voltage (RV)
0	3.342
25	3.800
30	3.853
40	3.807
50	3.942
60	3.630
75	3.202
100	3.073

In summary, low volume percent of ionic liquids would reduce stability of the lithium ions and ionic conductivity of GPE membrane; and high volume percent of ionic liquids would damage the protective layer on the surface of electrodes. An organic

electrolytes solution with the best battery performance turned out to be 1M LiPF₆ in 50 v% of ionic liquid, 25 v% EC, and 25 v% PC.

3.4 Conclusion

In previous figures and tables, adding ionic liquids in organic electrolytes solution increased the ionic conductivity, lower the solution resistance, higher the double-layer capacitance, and improved the charging and discharging performance. Combining all the factors, an organic electrolytes solution in the range of 50 v% of ILs is the most appropriate. In this entire system, EC and PC provided the protective film on the surface of electrodes and freed lithium ions from it compound; EMI-Tf increased the ionic conductivity and the stability of GPEs. In this work, EMI-Tf was applied as ionic liquids; besides this, other ionic liquids can also be introduced in an organic electrolytes solution, which would be discussed in the future.

REFERENCES

- [1] J. Y. Song, Y. Y. Wang, and C. C. Wan, "Review of gel-type polymer electrolytes for lithium-ion batteries," *Journal of Power Sources*, vol. 77, pp. 183-197, 1999.
- [2] E. Yoo, J. Kim, E. Hosono, H.-s. Zhou, T. Kudo, and I. Honma, "Large reversible Li storage of graphene nanosheet families for use in rechargeable lithium ion batteries," *Nano Letters*, vol. 8, pp. 2277-2282, 2008.
- [3] J. M. Tarascon and M. Armand, "Issues and challenges facing rechargeable lithium batteries," *Nature*, vol. 414, pp. 359-367, 2001.
- [4] M. Wakihara, "Recent developments in lithium ion batteries," *Materials Science and Engineering: R: Reports*, vol. 33, pp. 109-134, 2001.
- [5] A. Patil, V. Patil, D. Wook Shin, J.-W. Choi, D.-S. Paik, and S.-J. Yoon, "Issue and challenges facing rechargeable thin film lithium batteries," *Materials Research Bulletin*, vol. 43, pp. 1913-1942.
- [6] G. B. Appetecchi, P. Romagnoli, and B. Scrosati, "Composite gel membranes: a new class of improved polymer electrolytes for lithium batteries," *Electrochemistry Communications*, vol. 3, pp. 281-284, 2001.
- [7] M. Wachtler, D. Ostrovskii, P. Jacobsson, and B. Scrosati, "A study on PVdF-based SiO₂-containing composite gel-type polymer electrolytes for lithium batteries," *Electrochimica Acta*, vol. 50, pp. 357-361, 2004.
- [8] D. M. Esterly, "Manufacturing of Poly (vinylidene fluoride) and Evaluation of its Mechanical Properties," 2002.
- [9] V. Gentili, S. Panero, P. Reale, and B. Scrosati, "Composite gel-type polymer electrolytes for advanced, rechargeable lithium batteries," *Journal of Power Sources*, vol. 170, pp. 185-190, 2007.
- [10] A. Salimi and A. A. Yousefi, "Analysis Method: FTIR studies of β -phase crystal formation in stretched PVDF films," *Polymer Testing*, vol. 22, pp. 699-704, 2003.
- [11] J. R. Kim, S. W. Choi, S. M. Jo, W. S. Lee, and B. C. Kim, "Electrospun PVdF-based fibrous polymer electrolytes for lithium ion polymer batteries," *Electrochimica Acta*, vol. 50, pp. 69-75, 2004.

- [12] H. P. Zhang, P. Zhang, Z. H. Li, M. Sun, Y. P. Wu, and H. Q. Wu, "A novel sandwiched membrane as polymer electrolyte for lithium ion battery," *Electrochemistry Communications*, vol. 9, pp. 1700-1703, 2007.
- [13] G.-L. Ji, B.-K. Zhu, Z.-Y. Cui, C.-F. Zhang, and Y.-Y. Xu, "PVDF porous matrix with controlled microstructure prepared by TIPS process as polymer electrolyte for lithium ion battery," *Polymer*, vol. 48, pp. 6415-6425, 2007.
- [14] Y. Wang, J. Travas-Sejdic, and R. Steiner, "Polymer gel electrolyte supported with microporous polyolefin membranes for lithium ion polymer battery," *Solid State Ionics*, vol. 148, pp. 443-449, 2002.
- [15] F. Boudin, X. Andrieu, C. Jehoulet, and I. I. Olsen, "Microporous PVdF gel for lithium-ion batteries," *Journal of Power Sources*, vol. 81-82, pp. 804-807, 1999.
- [16] S. W. Choi, S. M. Jo, W. S. Lee, and Y. R. Kim, "An Electrospun Poly(vinylidene fluoride) Nanofibrous Membrane and Its Battery Applications," *Advanced Materials*, vol. 15, pp. 2027-2032, 2003.
- [17] R. Montazami, S. Liu, Y. Liu, D. Wang, Q. Zhang, and J. R. Heflin, "Thickness dependence of curvature, strain, and response time in ionic electroactive polymer actuators fabricated via layer-by-layer assembly," *JOURNAL OF APPLIED PHYSICS*, vol. 109, p. 104301, 2011.
- [18] R. Montazami, D. Wang, and J. R. Heflin, "Influence of conductive network composite structure on the electromechanical performance of ionic electroactive polymer actuators," *International Journal of Smart and Nano Materials*, vol. 3, pp. 204-213, 2012.
- [19] A. Manuel Stephan, "Review on gel polymer electrolytes for lithium batteries," *European Polymer Journal*, vol. 42, pp. 21-42, 2006.
- [20] B. Scrosati, "Recent advances in lithium ion battery materials," *Electrochimica Acta*, vol. 45, pp. 2461-2466, 2000.
- [21] B. Scrosati, F. Croce, and S. Panero, "Progress in lithium polymer battery R&D," *Journal of Power Sources*, vol. 100, pp. 93-100, 2001.
- [22] J. Song, Y. Wang, and C. Wan, "Review of gel-type polymer electrolytes for lithium-ion batteries," *Journal of Power Sources*, vol. 77, pp. 183-197, 1999.
- [23] A. Farnicola, B. Scrosati, and H. Ohno, "Potentialities of ionic liquids as new electrolyte media in advanced electrochemical devices," *Ionics*, vol. 12, pp. 95-102, 2006.

- [24] M. Egashira, H. Todo, N. Yoshimoto, and M. Morita, "Lithium ion conduction in ionic liquid-based gel polymer electrolyte," *Journal of Power Sources*, vol. 178, pp. 729-735, 2008.
- [25] K. Xu, "Nonaqueous liquid electrolytes for lithium-based rechargeable batteries," *Chemical reviews*, vol. 104, pp. 4303-4418, 2004.
- [26] H. Ye, J. Huang, J. J. Xu, A. Khalfan, and S. G. Greenbaum, "Li ion conducting polymer gel electrolytes based on ionic liquid/PVDF-HFP blends," *Journal of The Electrochemical Society*, vol. 154, pp. A1048-A1057, 2007.
- [27] C. Sirisopanaporn, A. Fernicola, and B. Scrosati, "New, ionic liquid-based membranes for lithium battery application," *Journal of Power Sources*, vol. 186, pp. 490-495, 2009.
- [28] T. Sato, S. Marukane, T. Narutomi, and T. Akao, "High rate performance of a lithium polymer battery using a novel ionic liquid polymer composite," *Journal of Power Sources*, vol. 164, pp. 390-396, 2007.
- [29] I. Krossing, J. M. Slattery, C. Daguene, P. J. Dyson, A. Oleinikova, and H. Weingärtner, "Why are ionic liquids liquid? A simple explanation based on lattice and solvation energies," *Journal of the American Chemical Society*, vol. 128, pp. 13427-13434, 2006.
- [30] H. Shobukawa, H. Tokuda, S.-I. Tabata, and M. Watanabe, "Preparation and transport properties of novel lithium ionic liquids," *Electrochimica acta*, vol. 50, pp. 305-309, 2004.
- [31] T. Tamura, K. Yoshida, T. Hachida, M. Tsuchiya, M. Nakamura, Y. Kazue, N. Tachikawa, K. Dokko, and M. Watanabe, "Physicochemical Properties of Glyme-Li Salt Complexes as a New Family of Room-temperature Ionic Liquids," *Chemistry Letters*, vol. 39, pp. 753-755, 2010.
- [32] T. Li and P. B. Balbuena, "Theoretical studies of lithium perchlorate in ethylene carbonate, propylene carbonate, and their mixtures," *Journal of The Electrochemical Society*, vol. 146, pp. 3613-3622, 1999.
- [33] H. Matsumoto, H. Sakaebe, K. Tatsumi, M. Kikuta, E. Ishiko, and M. Kono, "Fast cycling of Li/LiCoO₂ cell with low-viscosity ionic liquids based on bis (fluorosulfonyl) imide [FSI]⁺," *Journal of Power Sources*, vol. 160, pp. 1308-1313, 2006.
- [34] Y. Kumar, S. Hashmi, and G. Pandey, "Ionic liquid mediated magnesium ion conduction in poly (ethylene oxide) based polymer electrolyte," *Electrochimica acta*, vol. 56, pp. 3864-3873, 2011.

- [35] G. Pandey, Y. Kumar, and S. Hashmi, "Ionic liquid incorporated PEO based polymer electrolyte for electrical double layer capacitors: a comparative study with lithium and magnesium systems," *Solid State Ionics*, vol. 190, pp. 93-98, 2011.
- [36] K. Hayamizu, Y. Aihara, H. Nakagawa, T. Nukuda, and W. S. Price, "Ionic conduction and ion diffusion in binary room-temperature ionic liquids composed of [emim][BF₄] and LiBF₄," *The Journal of Physical Chemistry B*, vol. 108, pp. 19527-19532, 2004.
- [37] J. Li, K. Wilmsmeyer, J. Hou, and L. Madsen, "The role of water in transport of ionic liquids in polymeric artificial muscle actuators," *Soft Matter*, vol. 5, pp. 2596-2602, 2009.
- [38] J. Hou, Z. Zhang, and L. A. Madsen, "Cation/Anion Associations in Ionic Liquids Modulated by Hydration and Ionic Medium," *The Journal of Physical Chemistry B*, 2011.
- [39] G. Pandey and S. Hashmi, "Experimental investigations of an ionic-liquid-based, magnesium ion conducting, polymer gel electrolyte," *Journal of Power Sources*, vol. 187, pp. 627-634, 2009.
- [40] S. Rodrigues, N. Munichandraiah, and A. Shukla, "A review of state-of-charge indication of batteries by means of ac impedance measurements," *Journal of Power Sources*, vol. 87, pp. 12-20, 2000.
- [41] X. Wang, H. Hao, J. Liu, T. Huang, and A. Yu, "A novel method for preparation of macroporous lithium nickel manganese oxygen as cathode material for lithium ion batteries," *Electrochimica acta*, vol. 56, pp. 4065-4069, 2011.
- [42] M. A. Vorotyntsev, J.-P. Badiali, and G. Inzelt, "Electrochemical impedance spectroscopy of thin films with two mobile charge carriers: effects of the interfacial charging," *Journal of Electroanalytical Chemistry*, vol. 472, pp. 7-19, 1999.
- [43] D. K. Kim, P. Muralidharan, H.-W. Lee, R. Ruffo, Y. Yang, C. K. Chan, H. Peng, R. A. Huggins, and Y. Cui, "Spinel LiMn₂O₄ nanorods as lithium ion battery cathodes," *Nano letters*, vol. 8, pp. 3948-3952, 2008.
- [44] X. Li, F. Cheng, B. Guo, and J. Chen, "Template-synthesized LiCoO₂, LiMn₂O₄, and LiNi_{0.8}Co_{0.2}O₂ nanotubes as the cathode materials of lithium ion batteries," *The Journal of Physical Chemistry B*, vol. 109, pp. 14017-14024, 2005.

- [45] G. Appetecchi, F. Croce, A. De Paolis, and B. Scrosati, "A poly (vinylidene fluoride)-based gel electrolyte membrane for lithium batteries," *Journal of Electroanalytical Chemistry*, vol. 463, pp. 248-252, 1999.
- [46] P. Reale, S. Panero, and B. Scrosati, "Sustainable high-voltage lithium ion polymer batteries," *Journal of The Electrochemical Society*, vol. 152, pp. A1949-A1954, 2005.

CHAPTER 4

INFLUENCE OF GOLD NANOPARTICLES OF THE GEL POLYMER ELECTROLYTE

4.1 Introduction

Since the 1960s, lithium secondary batteries have been applied in mobile applications as power sources [1-3]. After years of previous effort, lithium secondary batteries, especially lithium-ion polymer batteries (LIPBs), are now the major power sources for portable electronic equipment such as mobile phones, laptops, electric vehicles, etc. [2] LIPBs rely on numerous advantages including low cost, reliability, and durability [4]. Nowadays, with the rapid development of electronic equipment, there is a greater demand for energy storage systems; and LIPBs can meet these needs [5, 6].

The design of a thin-film LIPB stands out among other LIPBs, because the thin-film features unique properties, which includes a wide variety of shapes, easy assembly, and flexible structure [7]. A thin-film LIPB typically consists of an anode, an electrolyte layer, and a cathode [8-11]. In the long term, the improvements on anodes, electrolytes, and cathodes are all necessary for progress in LIPBs. However, in the short term, the experiment discussed in this paper focuses on improving the Gel Polymer Electrolyte (GPE) by studying gold nanoparticle (AuNP) doped GPEs for flexible LIPB.

Currently, four polymers are identified as most suitable materials for the backbone structure of GPEs: polyethylene oxide (PEO), polyacrylonitrile (PAN), polymethyl methacrylate (PMMA), and polyvinylidene fluoride (PVdF) [12]. Based on

its excellent chemical stability, electrochemical properties, high affinity, and good mechanical properties, PVdF-based GPE is the most investigated structure for LIPBs [12-14]. Although exhibits promising performance, there is still room for improvement of PVdF-based GPEs. In order to form advanced GPEs, a group of researchers [15, 16] found that suitable ceramic fillers, such as silica, neutral alumina, acid alumina, and basic alumina, enhance the mechanical stability and allow a long and more efficient cycling of the battery. Metallic nanoparticles, mainly gold nanoparticles, are commonly used in diagnostics, sensors and other electronic devices, owing to gold is the most stable noble metal at the nano scale and gold has high electronic conductivity [17]. Based on quantum mechanical rules, the nanoparticles within diameter range 1-10nm would demonstrate electronic structures [18]. Gold nanoparticles with diameter 1-10nm are also considered as electrons, which have negative charge on the surface. The hypothesis of this work is that those negative charge carried by gold nanoparticles could attract lithium ions in the electrolytes to improve the performance of lithium ion polymer battery. To increase the ionic conductivity, reliability, and durability, gold nanoparticles are discussed as filler for GPE in this chapter.

Because of the polymer's polymorphism and PVdF's piezoelectric properties, lithium electrolytes can be stored in the approximately 50% amorphous structure, which is a result of PVdF having a semi-crystalline structure [9-11]. In this case, GPE is synthesized in two steps: fabricating porous PVdF membranes and then soaking the membranes in lithium electrolytes - lithium hexafluorophosphate (LiPF₆) in this work.

4.2 Experimental

Copper foil single-side coated by CMS Graphite (240mm L x 200mm W x 0.1mm t) was used as anode; aluminum foil single-side coated by LiMn₂O₄ (240mm L x 200mm W x 0.1mm t) was used as cathode (MTI Corporation). 1-Methyl-2-pyrrolidone (MP) (99.5%), ethylene carbonate (EC) (98%), propylene carbonate (PC) (99.7%), lithium hexafluorophosphate (LiPF₆) (98%), ethanol (99.5%), polyvinylidene fluoride (PVdF) were obtained from Sigma-Aldrich; gold nanoparticles (AUNPs) (diameter 3.2nm, 99.99%, 20ppm aqueous) were obtained from Purest Colloids Inc.

To make the AuNPs compatible with PVdF, the medium (water) was exchanged through a solvent exchange process as follow: Firstly, 100 mL original AuNPs solution was heated under 90°C. When the amount of solution decreased to 5mL, 1-Methyl-2-pyrrolidone (NMP) was added as the new solvent to increase the net volume to 25mL. The solution was heated again until 20mL was left. The solution was then sonicated for 60 minutes to re-disperse nanoparticles in the solution. Then the resultant solution, a 100ppm homogeneous AuNPs in NMP, was used for the experiments. Before and after the solvent exchange process, the property of solution was determined by ultraviolet absorbance spectroscopy.

The GPE is a membrane synthesized by trapping plasticizers EC PC in PVdF and NMP solutions and soaked in lithium hexafluorophosphate (LiPF₆). Firstly, EC and PC with weight ratio 1:1 was mixed and heated at 110°C to completely dissolution. Secondly, PVdF added to pure MP with weight ratio (1:3) as control group; and PVdF added to 40ppm AuNP-NMP solution with the same ratio as experimental group. When

the two solutions prepared individually, the first solution and the second solution with weight ratio 2:3 was heated together at 110°C and stirred on a magnetic stirrer until desired viscosity was reached. Then, the slurry was casted onto a flat glass disk. The flat glass disk with the slurry was then left at 80°C for 2 hours; then soaked into 10% ethanol solution for 12 hours. Then, a pale yellow membrane for as control and a light purple AuNP-doped membrane for the experiments remained in the glass disk. The membranes in both groups with 0.3mm thickness were cut into 22mm x 22mm square and were stored at ambient conditions. Finally, the membranes were activated by soaking into a 1M LiPF₆ dissolved in EC:PC (1:1) solution for 24 hours under Argon.

The ionic conductivity of GPE was measured by impedance spectroscopy (VersaSTAT 4) using two steel chips (15.5mm D x 0.2mm t) as the blocking electrode cells. Impedance spectroscopy (1.0E5 Hz to 0.1 Hz, $\Delta V = 10\text{mV}$) was periodically monitored over 30 days. The thin-film cell was assembled as shown in Figure 3; with GPE located in between the cathode and anode. In the actual model on the left of Figure 3, cathode and anode are exact 20mm x 20mm; but GPE film is larger than cathode and anode so the cell would not be shorted. The surface of protection cover that face inside of the cell is sticky, which helped airtight enclosure of the whole system. Charge-discharge was carried out with a computer controlled BST8-MA battery analyzer (MTI corporation), between 1V and 5V with a constant current of 0.5mA.

4.2 Results and discussion

4.2.1 Property of AuNPs:

The size of AuNPs used in this paper was sphere with diameter of 3.2nm. We used the Ultraviolet spectra to scan the samples: the original 20ppm AuNPs (medium: water) solution before evaporation (“before” in Figure 4.1), the 400ppm AuNPs (medium: water) solution after first evaporation (“only evaporate” in Figure 4.1), the final 100ppm AuNPs (medium: NMP) solution after second evaporation and ultrasonication (“after” in Figure 4.1). According to Mie theory, the optical absorption spectra directly depend on the size of nanoparticles: plasmon absorption bands of gold sphere nanoparticles solution with larger diameter would center at higher wavelength [19, 20]. Since the center of plasmon absorption bands (Figure 4.1) of AuNPs solution with water as medium kept constant (510nm) after first evaporation, the evaporation process did not affect the property of AuNPs. Meanwhile, AuNPs with higher concentration could absorb larger amount of Ultraviolet spectra, due to AuNPs with higher concentration would have more AuNPs in a unit volume solution; and the Ultraviolet spectra absorbance ability of each AuNP was the same. This indicated that the amount of absorbance of 400ppm AuNPs solution (1.8) was almost three times the amount of absorbance of the original 20ppm AuNPs solution (0.6).

For the spectrum of the final 100ppm AuNPs solution with NMP as medium, the shapes of its curves were similar to the other two and the peaks are approximately at the same wavelength, one can conclude that AuNPs have kept their unique properties in NMP. Nevertheless, by drawing a vertical line at the peak point of blue curve, it was

obvious that the peak of red curve shifts two minor units towards right. Also, the slope of red curves after the peak point was greater than the other two curves. Due to the center of plasmon absorption bands was representing the size of AuNPs [21-23], there were two probabilities: the size of AuNPs in the AuNPs NMP solution increased; and they slightly aggregated. Since the AuNPs is standard and stable by the introduction of the product, their size would not change. Thus, the only logical possibility is slight aggregating, in the other word, some of sphere AuNPs might gather and form a larger size sphere [24].

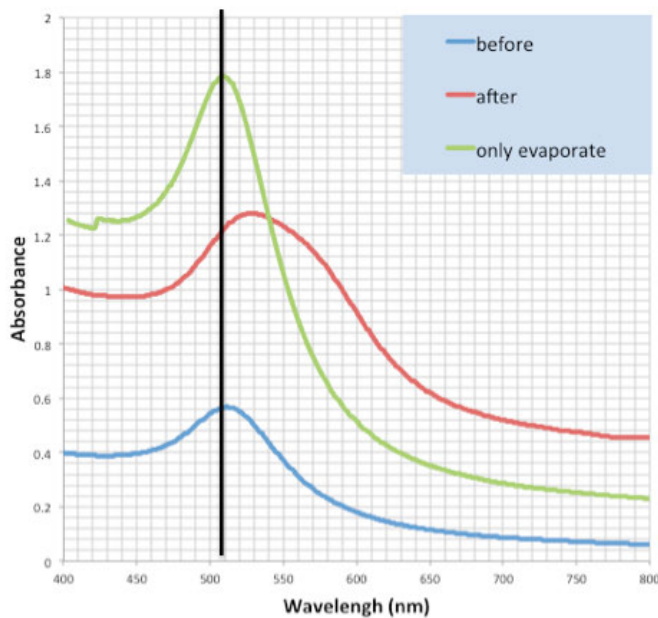


Figure 4.1 Comparison of the absorbance measured after solvent exchange (red line) with the absorbance measured before the solvent exchange (blue line) and absorbance measured by the AuNPs solution only evaporating

4.3.2 Ionic Conductivity:

At room temperature, GPE is placed between two steel chips as two blocking cells to measure the impedance. In high frequency range (100000Hz - 10000Hz), the

Nyquist plots act as a vertical line (Figure 4.2); and the effect of the imaginary part of impedance can be neglected.

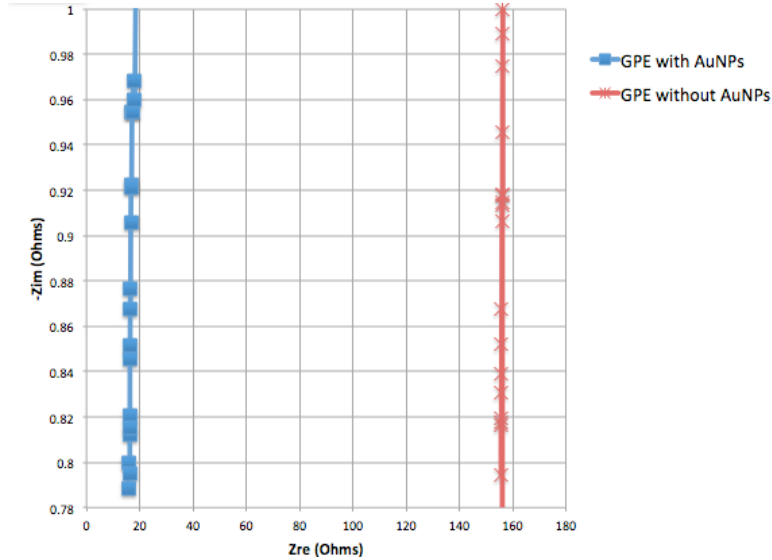


Figure 4.2 Comparison of the impedance for steel/GPE/steel with AuNPs and without AuNPs at high frequency

Then, after extending the vertical lines for both GPE with AuNPs and GPE without AuNPs, there are two intersecting points that meet the Z_{re} -axes. At the intersecting points, the value of real impedance can be written as the internal resistance. Also, the ionic conductivity (σ) is calculated by the Equation (1):

$$\sigma = \frac{t}{RA} \quad (1)$$

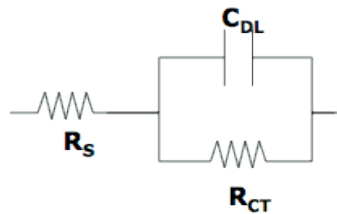
The value of each term for both GPE with AuNPs and GPE without AuNPs lists in Table 1. According to the data, the ionic conductivity of GPE with AuNPs ($0.96E-3$ S/cm) is much greater than the ionic conductivity of GPE without AuNPs ($1.18E-4$ S/cm). Because of AuNPs, shorter lithium ions' route in GPEs provides higher efficacy of the cell during the charging and discharging process.

Table 4.1 Values of each term in calculating ionic conductivity

Sample	t (mm)	R (ohm)	A (cm ²)	σ (S/cm)
GPE with AuNPs	0.31	17	1.89 cm ²	0.96 E-3
GPE without AuNPs	0.35	157	1.89 cm ²	1.18 E-4

4.3.3 Interfacial properties:

As Figure 7 showing, the Nyquist Plots for both cell with AuNPs and cell without AuNPs consist of semicircles. At high frequency and low frequency, the capacitive contribution is neglected; and it acts as pure resistance. Meanwhile, at the medium frequency, the semicircle reflects the most capacitive contribution. By assuming that semicircle is associated with parallel combination of interfacial resistance and the constant-phase element (CPE), the system of can use the equivalent circuit in Figure 6 to describe.

**Figure 4.3 Equivalent circuit of Lithium-ion polymer cell**

The solution resistance indicates the pure resistance at high frequency that also relates to bulk resistance of the polymer electrolyte; and the value of R_s locates in the left starting points in the Nyquist plots. R_s of the cell without AuNPs (200 Ohms) is approximately 100 times the cell with AuNPs (2 Ohms), which proves GPE with AuNPs has excellent conductivity comparing with the normal one. At low frequency, the value of the right ending points in the Nyquist plots is sum of charge-transfer resistance and

solution resistance. According to Nyquist plots, R_{ct} for cell without AuNPs is around 7300 Ohms; and R_{ct} for cell with AuNPs is around 145 Ohms. The double-layer capacitance can be calculated by Equation (2) and Equation (3).

$$f_m = \frac{f_h + f_l}{2} = \frac{1.0E5Hz + 0.1Hz}{2} = 50,000Hz \quad (2)$$

$$C_{DL} = \frac{2\pi}{f_m Z_{im,m}} \quad (3)$$

In this case, estimated CDL for cell without AuNPs (46.5nF) is significantly smaller than estimated CDL for AuNPs (2.28 μ F). Higher capacitance indicates more energy can be stored in each individual cell. In the parallel combination of double-layer capacitance and charge-transfer resistance, the lithium-ion polymer cell with AuNPs with lower internal resistance and higher capacitance in a certain size improves the performance of the whole battery.

From the Nyquist plots, the diameter of each semicircle shrinks and then extends over time. In the first few days, it takes time for LiPF₆ flooding the half amorphous structure; also the cell is not fully discharged. Between day 4 and day 7, there exists the smallest diameter for both cases. In the end of the month, the diameter reaches the largest value due to small amount of PVdF is dried. In day 30, the curve of cells with AuNPs is not as smooth as other. As this paper mentioned before, aggregating is one of the issue in this work; so in long term it will infinitesimally affect the performance of the cell.

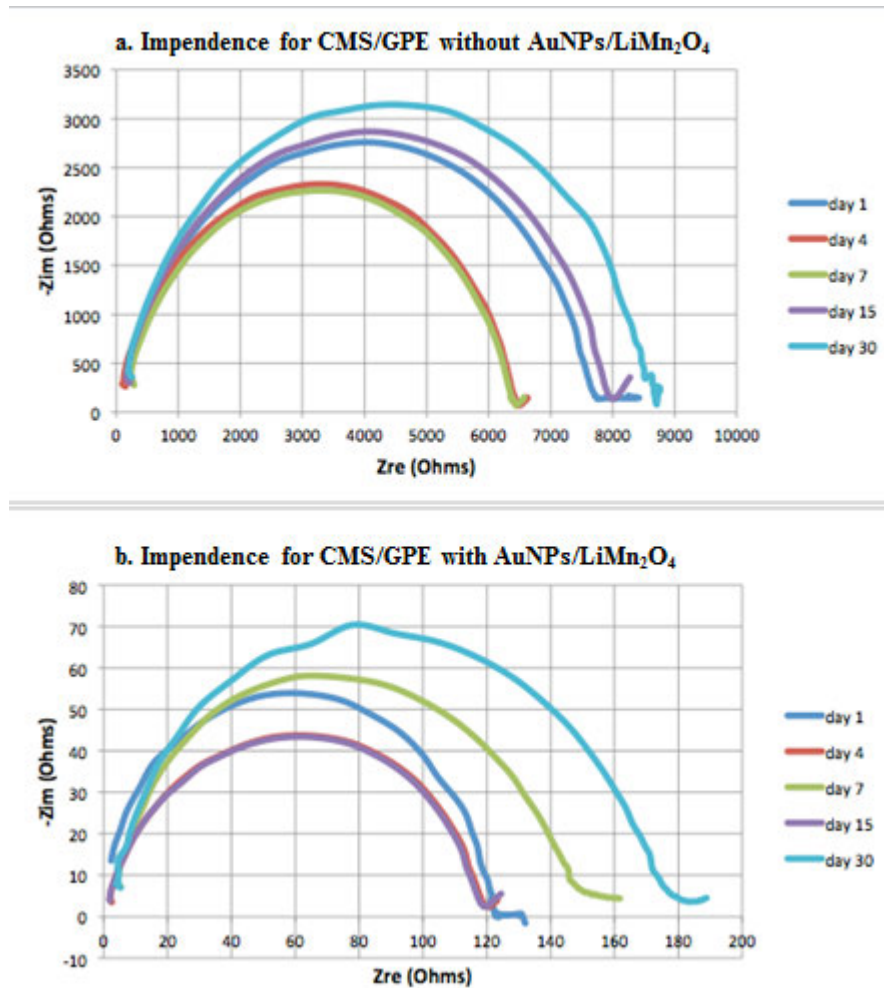


Figure 4.4 a) Nyquist plots obtained for LIPB with AuNPs for 1 month at room temperature, b) Nyquist plots obtained for LIPB with AuNPs for 1 month at room temperature

4.3.4 Battery performance:

Galvan static charging and discharging were used to evaluate to performance of the entire system (CMS/GPE/LiMn₂O₄). Each cycle included constant current (0.5C) discharging, rest (5mins), constant current charging and constant voltage charging in the voltage range of 0.5V – 5V. During each process, the Battery Analyzer monitored the current, voltage, and capacities every 5 seconds.

The average rest voltages could represent the battery performance after fully charged and the value of charging/discharging capacity along shelf life. The average rest voltage of GPE with AuNPs (RV=3.8V) is higher than the average rest voltage of GPE without AuNPs (RV=3.3V). A higher average rest voltage indicated that the cell could operate a higher potential voltage during discharges [16].

Figure 4.5 compared the cycling stability of each battery system. After adding AuNPs as filler in GPE, both charging capacity and discharging capacity during 50 charging/discharging cycles were increased 30% comparing with the GPE without AuNPs. The charging/discharging capacity indicated the energy storage ability of each cell. In this case, the materials of cathodes and anodes are exactly the same; so are the assembly condition and assembly process. Then, higher charging/discharging capacity in this case implied that GPE with AuNPs stored more energy; in the other word, more liquids electrolytes (LiPF_6) solution was stored inside of GPE membrane [13, 14, 25]. According to the information provided by the Purest Colloids Inc., AuNPs used in this paper had negative charges on the surface. A small amount of AuNPs within the GPE membrane is highly possible to generate an electronic field that could attract more Lithium ions during activation process. Then, GPE membrane with AuNPs could provide and transmit more lithium ions during the chemical reaction happened between cathode and anode. In this case, AuNPs did enhance the performance of Lithium ion polymer battery by storing more lithium ions to increase the charging/discharging capacity and operate higher potential voltage.

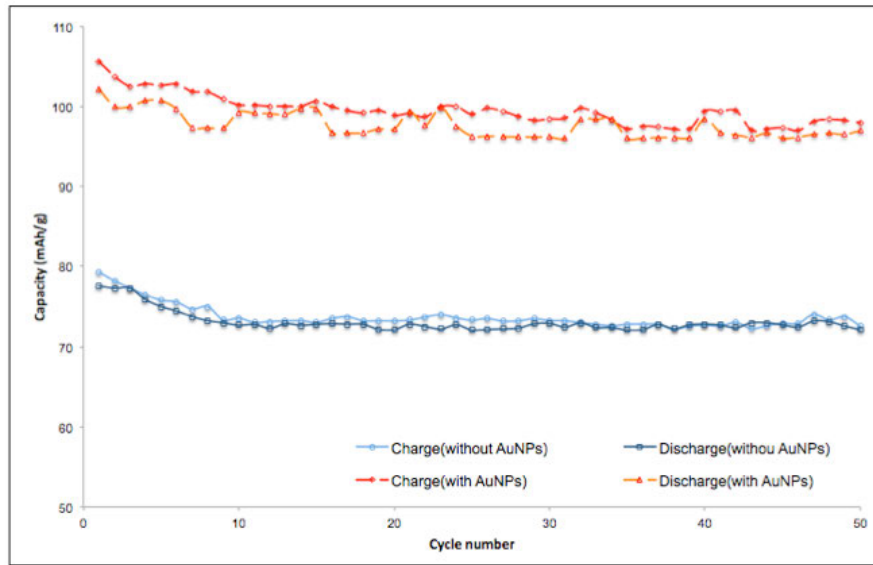


Figure 4.5 Consecutive cycling behavior of CMS/GPE with or without AuNPs/LiMn₂O₄ systems

4.4 Conclusion

The GPE is a membrane synthesized by trapping ethylene carbonate, and propylene carbonate in polyvinylidene fluoride and 1-methyl-2-pyrrolidinone solutions. Besides applying phase transfer method, gold nanoparticles are added in gel polymer electrolyte as fillers, which enhance the ionic conductivity and the performance of the whole battery. After applying the AuNPs, the ionic conductivity of gel polymer electrolyte increased 10 times the general GPE. As part of lithium-ion polymer cell, the gel polymer electrolyte with AuNPs led to higher capacity and lower internal resistance. Even if there exist aggregating, the amount is so small that it can be neglected.

REFERENCES

- [1] D. Wainwright, "Battery incorporating hydraulic activation of disconnect safety device on overcharge," ed: Google Patents, 1995.
- [2] A. Patil, V. Patil, D. Wook Shin, J.-W. Choi, D.-S. Paik, and S.-J. Yoon, "Issue and challenges facing rechargeable thin film lithium batteries," *Materials research bulletin*, vol. 43, pp. 1913-1942, 2008.
- [3] J. S. Lundsgaard, "Electrochemical cell," ed: Google Patents, 1989.
- [4] J. M. Tarascon and M. Armand, "Issues and challenges facing rechargeable lithium batteries," *Nature*, vol. 414, pp. 359-367, 2001.
- [5] A. S. Aricò, P. Bruce, B. Scrosati, J.-M. Tarascon, and W. Van Schalkwijk, "Nanostructured materials for advanced energy conversion and storage devices," *Nature materials*, vol. 4, pp. 366-377, 2005.
- [6] A. Manthiram, A. V. Murugan, A. Sarkar, and T. Muraliganth, "Nanostructured electrode materials for electrochemical energy storage and conversion," *Energy & Environmental Science*, vol. 1, pp. 621-638, 2008.
- [7] W. H. Meyer, "Polymer Electrolytes for Lithium - Ion Batteries," *Advanced materials*, vol. 10, pp. 439-448, 1998.
- [8] E. Peled, C. Menachem, D. Bar - Tow, and A. Melman, "Improved Graphite Anode for Lithium - Ion Batteries Chemically Bonded Solid Electrolyte Interface and Nanochannel Formation," *Journal of The Electrochemical Society*, vol. 143, pp. L4-L7, 1996.
- [9] M. Wakihara, "Recent developments in lithium ion batteries," *Materials Science and Engineering: R: Reports*, vol. 33, pp. 109-134, 2001.
- [10] R. Kanno, Y. Takeda, T. Ichikawa, K. Nakanishi, and O. Yamamoto, "Carbon as negative electrodes in lithium secondary cells," *Journal of Power Sources*, vol. 26, pp. 535-543, 1989.
- [11] M. Mohri, N. Yanagisawa, Y. Tajima, H. Tanaka, T. Mitate, S. Nakajima, M. Yoshida, Y. Yoshimoto, T. Suzuki, and H. Wada, "Rechargeable lithium battery based on pyrolytic carbon as a negative electrode," *Journal of Power Sources*, vol. 26, pp. 545-551, 1989.

- [12] M. Armand and J.-M. Tarascon, "Building better batteries," *Nature*, vol. 451, pp. 652-657, 2008.
- [13] A. Manuel Stephan, "Review on gel polymer electrolytes for lithium batteries," *European Polymer Journal*, vol. 42, pp. 21-42, 2006.
- [14] J. Song, Y. Wang, and C. Wan, "Review of gel-type polymer electrolytes for lithium-ion batteries," *Journal of Power Sources*, vol. 77, pp. 183-197, 1999.
- [15] V. Gentili, S. Panero, P. Reale, and B. Scrosati, "Composite gel-type polymer electrolytes for advanced, rechargeable lithium batteries," *Journal of Power Sources*, vol. 170, pp. 185-190, 2007.
- [16] H. Wang, H. Huang, and S. L. Wunder, "Novel Microporous Poly (vinylidene fluoride) Blend Electrolytes for Lithium - Ion Batteries," *Journal of The Electrochemical Society*, vol. 147, pp. 2853-2861, 2000.
- [17] J. Shan and H. Tenhu, "Recent advances in polymer protected gold nanoparticles: synthesis, properties and applications," *Chemical Communications*, pp. 4580-4598, 2007.
- [18] M.-C. Daniel and D. Astruc, "Gold nanoparticles: assembly, supramolecular chemistry, quantum-size-related properties, and applications toward biology, catalysis, and nanotechnology," *Chemical Reviews*, vol. 104, pp. 293-346, 2004.
- [19] S. Link and M. A. El-Sayed, "Size and temperature dependence of the plasmon absorption of colloidal gold nanoparticles," *The Journal of Physical Chemistry B*, vol. 103, pp. 4212-4217, 1999.
- [20] K. Koga, T. Ikeshoji, and K.-i. Sugawara, "Size-and temperature-dependent structural transitions in gold nanoparticles," *Physical Review Letters*, vol. 92, p. 115507, 2004.
- [21] S. K. Ghosh and T. Pal, "Interparticle coupling effect on the surface plasmon resonance of gold nanoparticles: from theory to applications," *Chemical Reviews*, vol. 107, pp. 4797-4862, 2007.
- [22] K.-H. Su, Q.-H. Wei, X. Zhang, J. Mock, D. R. Smith, and S. Schultz, "Interparticle coupling effects on plasmon resonances of nanogold particles," *Nano letters*, vol. 3, pp. 1087-1090, 2003.
- [23] J. Aizpurua, P. Hanarp, D. Sutherland, M. Käll, G. W. Bryant, and F. G. De Abajo, "Optical properties of gold nanorings," *Physical Review Letters*, vol. 90, p. 057401, 2003.

- [24] N. Malikova, I. Pastoriza-Santos, M. Schierhorn, N. A. Kotov, and L. M. Liz-Marzán, "Layer-by-layer assembled mixed spherical and planar gold nanoparticles: control of interparticle interactions," *Langmuir*, vol. 18, pp. 3694-3697, 2002.
- [25] J.-M. Tarascon and M. Armand, "Issues and challenges facing rechargeable lithium batteries," *Nature*, vol. 414, pp. 359-367, 2001.

CHAPTER 5

Conclusion and Future Prospective

Nowadays, due to numerous advantages of this class of batteries, including a wide variety of possible cell shape, reliability, and durability, lithium-ion polymer batteries are widely established as power sources for portable electronic equipment such as mobile phones and laptops, as well as hybrid and electric vehicles [1-8]. This work investigates and presents two methods to improve the gel polymer electrolyte efficiency in lithium ion polymer batteries by introducing ionic liquids and gold nanoparticles. The gel polymer electrolyte is a membrane synthesized by trapping ethylene carbonate, and propylene carbonate in polyvinylidene fluoride and 1-methyl-2-pyrrolidinone solutions, which is then activated in lithium salt with organic solvent solution. Adding ionic liquids to the organic solvent increases the ionic conductivity, lowers the solution resistance, and enhances the double-layer capacitance, and improves the charging and discharging performance. Combining all the factors, an organic electrolytes solution containing approximately 50-volume% of ILs is the most efficient. Gold nanoparticles are added in gel polymer electrolyte as fillers, which also enhance the ionic conductivity and the performance of the battery as a whole.

This thesis discussed two ways, added ionic liquids as the solvent of LiPF_6 and added AuNPs in GPE membrane, to improve the performance of Lithium ion polymer battery, however, it has not reported the results of combining two methods. In the future, I am planning to compare the Lithium ion polymer battery with both ionic liquid and

AuNPs with the one with only one additive. It is highly possible that GPE with both ionic liquid and AuNPs will have higher ionic conductivity and larger capacity. Also, the minor problem of AuNPs aggregation during solvent exchange process needs to be addressed in the future. As I am concerned, add some coating on the surface of AuNPs or use a different size of AuNPs might solve the AuNPs aggregation problem.

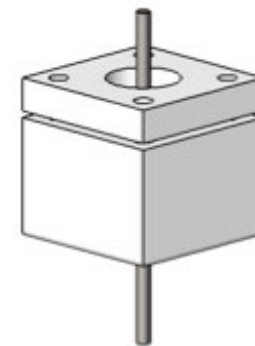
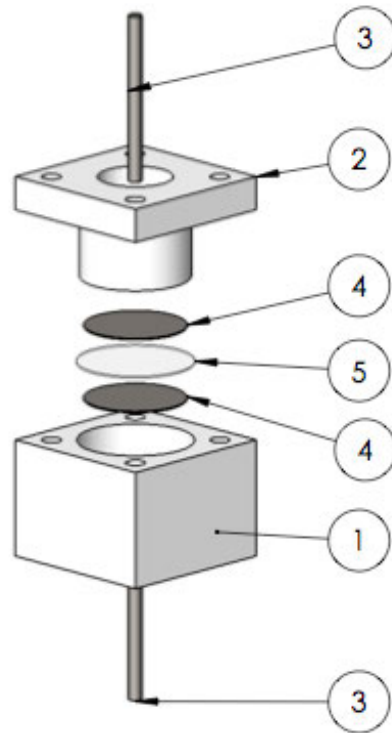
The advantage of lithium-ion polymer batteries discussed in this thesis is the polymer electrolytes. The gel polymer or solid polymer electrolytes allow a wide variety of designs and provide means for complex nano and micro-structures which in turn can improve performance of the device. These structural properties could not be achieved in liquid cells.

REFERENCES

- [1] J. Besenhard and G. Eichinger, "High energy density lithium cells: Part I. Electrolytes and anodes," *Journal of Electroanalytical Chemistry and Interfacial Electrochemistry*, vol. 68, pp. 1-18, 1976.
- [2] J.-P. Gabano, "Lithium batteries," *London and New York, Academic Press, 1983, 467 p.*, vol. 1, 1983.
- [3] W. H. Meyer, "Polymer Electrolytes for Lithium - Ion Batteries," *Advanced materials*, vol. 10, pp. 439-448, 1998.
- [4] M. Mohri, N. Yanagisawa, Y. Tajima, H. Tanaka, T. Mitate, S. Nakajima, M. Yoshida, Y. Yoshimoto, T. Suzuki, and H. Wada, "Rechargeable lithium battery based on pyrolytic carbon as a negative electrode," *Journal of Power Sources*, vol. 26, pp. 545-551, 1989.
- [5] A. Patil, V. Patil, D. Wook Shin, J.-W. Choi, D.-S. Paik, and S.-J. Yoon, "Issue and challenges facing rechargeable thin film lithium batteries," *Materials research bulletin*, vol. 43, pp. 1913-1942, 2008.
- [6] J. M. Tarascon and M. Armand, "Issues and challenges facing rechargeable lithium batteries," *Nature*, vol. 414, pp. 359-367, 2001.
- [7] W. van Schalkwijk and B. Scrosati, *Advances in lithium-ion batteries*: Springer, 2002.
- [8] M. Wakihara, "Recent developments in lithium ion batteries," *Materials Science and Engineering: R: Reports*, vol. 33, pp. 109-134, 2001.

APPENDIX

ITEM NO.	PART NUMBER	Material	QTY.
1	bottom	Plastic (PVC)	1
2	top	Plastic (PVC)	1
3	bar	Alloys Steel (SS)	2
4	steel chip	Alloys Steel (SS)	2
5	GPE	PVdF	1



PROPRIETARY AND CONFIDENTIAL
 THE INFORMATION CONTAINED IN THIS DRAWING IS THE SOLE PROPERTY OF <INSERT COMPANY NAME HERE>. ANY REPRODUCTION IN PART OR AS A WHOLE WITHOUT THE WRITTEN PERMISSION OF <INSERT COMPANY NAME HERE> IS PROHIBITED.

		UNLESS OTHERWISE SPECIFIED:	NAME	DATE	TITLE: Test Cell (SS)
		DIMENSIONS ARE IN INCHES TOLERANCES: FRACTIONAL ± ANGULAR: MACH ± BEND ± TWO PLACE DECIMAL ± THREE PLACE DECIMAL ±	DRAWN Ruisi		
		INTERPRET GEOMETRIC TOLERANCING PER:	CHECKED		
		MATERIAL	ENG APPR.		
			MFG APPR.		
			Q.A.		
			COMMENTS:		
NEXT ASSY	USED ON	FINISH			SIZE DWG. NO. REV A Assem
APPLICATION		DO NOT SCALE DRAWING			SCALE: 1:2 WEIGHT: SHEET 1 OF 1

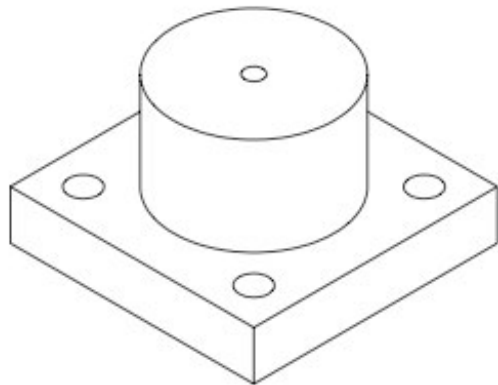
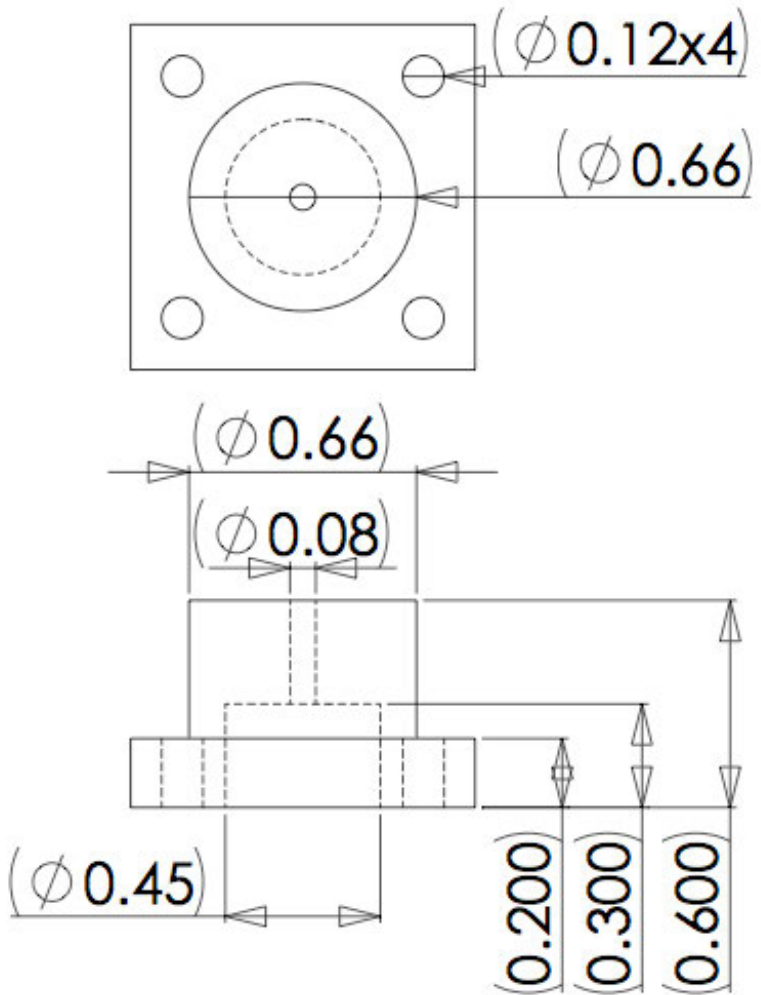
5

4

3

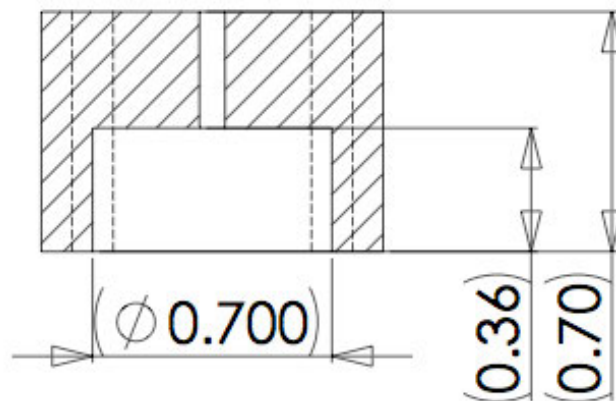
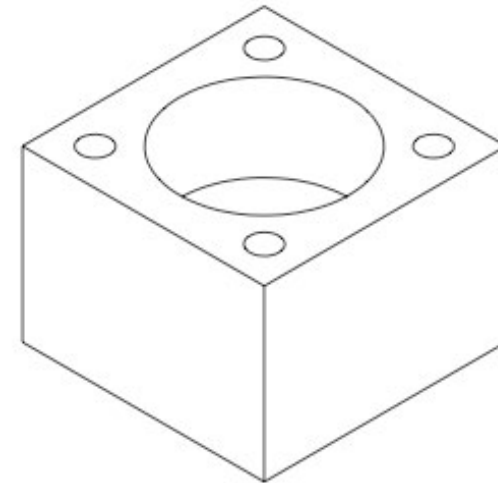
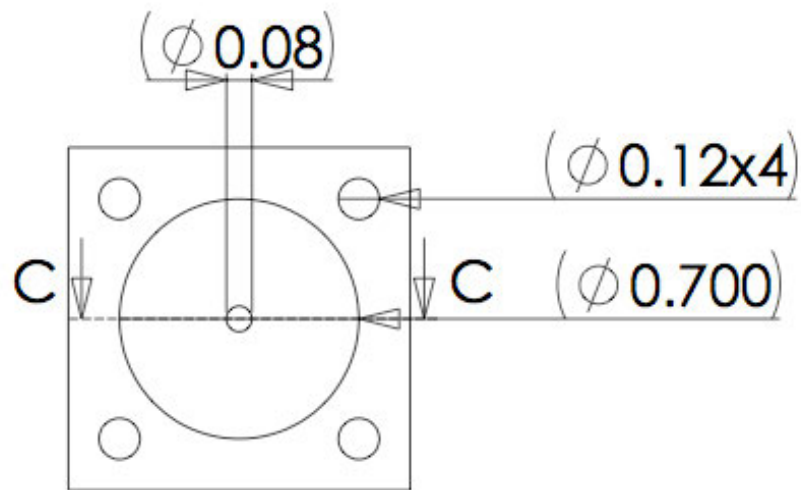
2

1



PROPRIETARY AND CONFIDENTIAL
 THE INFORMATION CONTAINED IN THIS
 DRAWING IS THE SOLE PROPERTY OF
 <INSERT COMPANY NAME HERE>. ANY
 REPRODUCTION IN PART OR AS A WHOLE
 WITHOUT THE WRITTEN PERMISSION OF
 <INSERT COMPANY NAME HERE> IS
 PROHIBITED.

		DIMENSIONS ARE IN INCHES		NAME		DATE		Unit: inch	
		TOLERANCES:		DRAWN					
		FRACTIONAL ±		CHECKED					
		ANGULAR: MACH ± BEND ±		ENG APPR.					
		TWO PLACE DECIMAL ±		MFG APPR.					
		THREE PLACE DECIMAL ±		Q.A.					
		MATERIAL						Top	
		FINISH							
NEXT ASSY	USED ON							SIZE DWG. NO.	
APPLICATION		DO NOT SCALE DRAWING						REV.	
						SCALE: 2:1		WGT:	
								SHEET 1 OF 1	



SECTION C-C

PROPRIETARY AND CONFIDENTIAL
 THE INFORMATION CONTAINED IN THIS
 DRAWING IS THE SOLE PROPERTY OF
 <INSERT COMPANY NAME HERE>. ANY
 REPRODUCTION IN PART OR AS A WHOLE
 WITHOUT THE WRITTEN PERMISSION OF
 <INSERT COMPANY NAME HERE> IS
 PROHIBITED.

		DIMENSIONS ARE IN INCHES TOLERANCES: FRACTIONAL ± ANGULAR: MACH ± BEND ± TWO PLACE DECIMAL ± THREE PLACE DECIMAL ±	DRAWN	NAME	DATE	Unit: Inch
			CHECKED			
			ENG APPR.			
			MFG APPR.			
			Q.A.			
		MATERIAL	---			bottom
		FINISH	---			
NEXT ASSY	USED ON			SIZE	DWG. NO.	REV.
APPLICATION	DO NOT SCALE DRAWING			A		
		SCALE: 2:1	WEIGHT:		SHEET 1 OF 1	